SECURITY CLASSIFICATION OF THIS PAGE (When Data Entered)

REPORT DOCUMENTATION PAGE

READ INSTRUCTIONS BEFORE COMPLETING FORM

1. REPORT NUMBER: NR 202-246	2. GOVT ACCESSION NO.
3. RECIPIENT'S CATALOG NUMBER	
4. TITLE (and Subtitle): Characterization of Transverse Tubule Vesicles Isolated from Skeletal Muscle	5. TYPE OF REPORT & PERIOD COVERED: Final 7/1/82 - 9/30/84 Report
6. PERFORMING ORG. REPORT NUMBER: G37136	
7. AUTHOR(s): Troy J. Beeler, Ph.D.	8. CONTRACT OR GRANT NUMBER(s): N00014-82-WR-2027 0
9. PERFORMING ORGANIZATION NAME AND ADDRESS: Troy J. Beeler, Dept. of Biochemistry, USUHS, 4301 Jones Bridge Rd, Bethesda, MD 20814-4799	10. PROGRAM ELEMENT, PROJECT, TASK AREA & WORK UNIT NUMBERS: 61153N
11. CONTROLLING OFFICE NAME AND ADDRESS: Chief of Naval Research, Code 512, Arlington, VA 22217	12. REPORT DATE: 20 Aug 84
	13. NUMBER OF PAGES
14. MONITORING AGENCY NAME & ADDRESS (if different from Controlling Office)	15. SECURITY CLASS. (of this report): Unclassified
	15a. DECLASSIFICATION/DOWNGRADING SCHEDULE

16. DISTRIBUTION STATEMENT (of this Report)

A Approved for public release; distribution unlimited

17. DISTRIBUTION STATEMENT (of the abstract entered in Block 20, if different from Report)

18. SUPPLEMENTARY NOTES

19. KEY WORDS (Continue on reverse side if necessary and identify by block number)

Muscle	Excitation-Contraction Coupling
Contraction	Ca^{2+}
Sarcoplasmic reticulum	Ca^{2+} release
Transverse Tubule	Ca^{2+} transport

20. ABSTRACT (Continue on reverse side if necessary and identify by block number)

Muscle contraction is initiated by the release of Ca^{2+} from the sarcoplasmic reticulum following depolarization of the transverse tubule by the action potential. In order to learn more about the molecular mechanism of the excitation contraction coupling process, we have isolated T-tubule vesicles, sarcoplasmic reticulum vesicles derived from the terminal cisternae, and intact triad junctions in which the T-tubule and sarcoplasmic reticulum

(Continued on reverse)

DD FORM 1 JAN 73 1473 EDITION OF 1 NOV 65 IS OBSOLETE

S/N 0102-LF-014-6601

SECURITY CLASSIFICATION OF THIS PAGE (When Data Entered)

Block #20 - Continued

membranes remain attached. The lipid and protein composition of the T-tubule vesicles differ greatly from that of the sarcoplasmic reticulum membrane. The T-tubule membrane is highly enriched in certain proteins which have a molecular weight of 220,000, 140,000, 70,000, 32,000 and 28,000. The sarcoplasmic reticulum vesicles derived from the terminal cisternae are enriched in 2 proteins with molecular wts of 320,000 and 350,000. The role that these proteins may have in excitation-contraction coupling is not known. More than 15% of the protein in the T-tubule membrane binds to wheat germ agglutinin indicating a large proportion of glycoproteins while less than 1% of sarcoplasmic reticulum membrane proteins bind to wheat germ agglutinin. The cholesterol content of T-tubule was 10X that of sarcoplasmic reticulum. The permeability of the T-tubule membrane to monovalent and divalent cations was lower than that of the sarcoplasmic reticulum. The permeability of the T-tubule vesicles to K^+ was higher than that of Na^+ allowing of a resting membrane potential by K gradients. The Ca^{2+} permeability of T-tubule vesicles was very low. The Ca-ATPase activity of the T-tubule vesicle was at least 100 fold lower that that of the sarcoplasmic reticulum. The T-tubule membrane was unusually high in Mg-ATPase activity (10-20 μmol/mg min). The properties of the Mg-ATPase differed from those described for the Na, K-ATPase, Ca,Mg-ATPase, myosin ATPase and the mitochondrial F_1 ATPase. The Mg-ATPase was inactivated by ATP. This inactivation was prevented by cross-linking the membrane proteins with lectins, antibodies or chemical cross linkers. This enzyme was not specific for the T-tubule but also found in the plasma membrane of other cells. The sarcoplasmic reticulum membrane contains a Ca^{2+} channel which is activated by Ca^{2+} (Ca^{2+}-induced Ca^{2+} release). Activation of this channel requires ATP and KCl (or similar salt); is inhibited by Mg^{++} and rutherium red; and is greatly enhanced by halothane. The T-tubule membrane contains a voltage-gated Ca^{2+} channel which binds the Ca^{2+} channel blocker nitrendipine. The Ca^{2+} channel constitutes about 1% of the T-tubule protein but its role in excitation-contraction coupling has yet to be clarified.

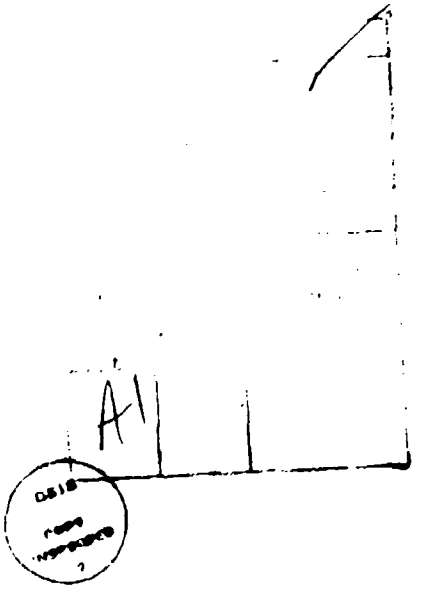

Characterization of Transverse Tubule Vesicles Isolated From Skeletal Muscle

Final Report 7/1/82--9/30/84

Introduction

Muscle contraction is initiated by the release of Ca from the sarcoplasmic reticulum following depolarization of the T-tubule (transverse tubule) by the action potential which is generated at the neuromuscular junction.

The purpose of this research as originally stated was to

1. Isolate T-tubule vesicles from rat skeletal muscle,

2. Characterization of the protein, lipid, and carbohydrate content of T-tubule vesicles,

3. Identify T-tubule specific proteins,

4. Characterize the excitability of isolated T-tubule vesicles,

5. Investigate the interaction between T-tubule vesicles with sarcoplasmic reticulum vesicles.

The overall goal is to increase our understanding of the excitation-contraction coupling process by isolating the membranes involved in the Ca release process and study their functional and physical properties. This report covers the results that have been obtained in our laboratory in the last two years.

Isolation of T-tubule Membrane

T-tubule membranes from rat skeletal muscle have been prepared by three methods.

Method 1. Triads (T-tubule and sarcoplasmic reticulum vesicle still attached) are first isolated from the mitochondrial fraction using density gradient centrifugation on sucrose and Percoll gradients. The T-tubule is then separated from the terminal cisternae by French press treatment followed by sucrose gradient centrifugation.

Method 2. T-tubule vesicles can also be prepared from the microsomal fraction (1). The microsomes are fractionated by 2 successive sucrose gradient centrifugations. The low density vesicles obtained at the 10-27% sucrose interface of the second gradient have a high content of cholesterol, Na^+,K^+-ATPase, glycoproteins, and nitrendipine-binding sites and therefore are beleived to consist of T-tubule vesicles although there may also be plasma membrane present. These T-tubule vesicles may be freed from the terminal cisternae of the sarcoplasmic reticulum during the homogenization of the muscle or may consist of non-junctional T-tubule membrane.

Method 3. The last method used to prepare T-tubule membranes is similiar to method 2 except the muscle is treated with .5 M LiBr, 50 mM Tris (pH 8.5) to remove the actin-myosin fibers. The yield of T-tubule membrane

obtained by this method was 10 times that of the other methods but the vesicles were "leaky" after the LiBr treatment.

The protein composition of the T-tubule vesicles prepared by the 3 methods was similar with major proteins having molecular weights of 220 000, 140 000, 70 000, 32 000 and 28 000. Other proteins were found enriched in one preparation but low in another. The significance of this is not known.

ATPase activity of T-tubule Membrane (1)

The Ca-ATPase mediates the transport of Ca and is the major protein found in the sarcoplasmic reticulum membrane. The Ca-ATPase activity in the T-tubule vesicle is at least 100 times less than that of the sarcoplasmic reticulum. On the otherhand, the basal Mg-ATPase activity was very high in the T-tubule membrane. This ATPase was found to have some very interesting and unique properties. The rate of ATP hydrolysis by the Mg^{2+}-ATPase was nonlinear but declined exponentially. The inactivation of the Mg^{2+}-ATPase was dependent on the presence of ATP or its analogue AMPPNP. Wheat germ agglutinin, concanavalin A, antiserum or cross-linking reagents such as glutaraldehyde could prevent inactivation. Detergents at low concentration accelerated the rate of inactivation but did not significantly influence the initial rate of ATP hydrolysis. This data indicate that the inactivation of the Mg^{2+}-ATPase by ATP requires the mobility of the membrane protein. Cross-linking the membrane proteins with lectins, antiserum or glutaraldehyde blocks inactivation; increasing the memberane fluidity with detergents increases the rate of inactivation.

The function of the Mg^{2+}-ATPase is not known but an enzyme with similar properties was found in brain, kidney, spleen, lung, heart, liver and adipose tissue.

The T-tubule membrane was also enriched in Na,K-ATPase activity which could not be detected in the sarcoplasmic reticulum membrane.

Ion (Na, K, Ca) permeability of T-tubule vesicles

The regulation of ion fluxes across the T-tubule membrane is closely related to the excitation-contraction coupling process. The T-tubule membrane contains both voltage-gated Na^+ and Ca^{2+} channels and transport systems that maintain the Na^+, K^+, and Ca^{2+} gradients across the membrane. We have measured the resting membrane potential of T-tubule vesicles generated by K^+ gradients using voltage sensitive optical probes. The isolated Ttubule vesicle had a K^+ permeability that was at least 10 times that of Na. The Ca^{2+} permeability was very low ($t_{1/2}$ =15 min) despite the presence of the voltage gated Ca channel. Attempts to activate the Ca channel by altering the membrane potential of with BayK 8644 was unsuccessful. Inactivation of the Ca channel when removed from the cell is a common observation. It is likely that some metabolite or factor from the cell is required for activation.

Ca release from Triad junctions

Sarcoplasmic reticulum can be separated into several subfractions; low-density sarcoplasmic reticulum vesicles, high density sarcoplasmic reticulum vesicles and triad junctions.

The low-density and high-density sarcoplasmic reticulum vesicles are obtained by separating the microsomal fraction by sucrose gradient centrifugation. The high density sarcoplasmic reticulum vesicles are presumably derived from the terminal cisternae while the low-density sarcoplasmic reticulum vesciles are believed to be derived from the nonjunctional sarcoplasmic reticulum. The triad junctions are obtained from 1000-15000 g fraction. The mitochondrial and myofibril contamination is removed form the triad junctions by centrifugation on Percoll and sucrose gradients. Low concentrations of Halothane (.1-.5mM) induce the release of Ca^{2+} from the high density sarcoplasmic reticulum vesicles and the triad junction fractions but does not affect Ca^{2+} accumulation by the low-density sarcoplasmic reticulum. Nor does this concentration of Halothane induce the release of Ca^{2+} from liposomes prepared with lipids extracted from heavy sarcoplasmic reticulum vesicles. Halothane-induced Ca^{2+} release required ATP and was inhibited by Mg^{2+} (1-10 mM) and ruthenium red (.5-2 μM). The data suggest that Ca^{2+} release is induced by Halothane at specific sites on the sarcoplasmic reticulum membrane and that these sites are probably in the terminal cisternae. This raises the possibility the Halothane-induced Ca^{2+} release occurs at the same site which releases Ca^{2+} during excitation-contraction coupling. The mechanism by which Halothane initiates Ca^{2+} release from sarcoplasmic reticulum vesicles may be the same mechanism by which Halothane induces malignant hyperthermia in susceptible individuals. Malignant hyperthermia is beleived to be caused by increased Ca^{2+}release from the sarcoplasmic reticulum.

Ca^{2+} also induces the release of Ca^{2+} from the isolated triad (Ca^{2+}-induced Ca^{2+} release). This Ca^{2+} activated Ca release has the same properties as the Halothane-induced Ca^{2+} release. Indeed, the Halothane-induced Ca^{2+} release required the presence of external Ca^{2+}. Therefore, it is likely that Ca^{2+}-induced Ca^{2+} release and the Halothane-induced Ca release are mediated by the same system.

Other studies

Effect of Na_3VO_4 and Membrane Potential on the Structure of Sacroplasmic Reticulum Membrane(2)

Two-dimensional crystalline arrays of Ca^{2+}-ATPase molecules develop after treatment of sarcoplasmic reticulum vesicles with Na_3VO_4 in a Ca^{2+}-free medium. The influence of membrane potential upon the rate of crystallization was studied by ion substitution using oxonol VI and 3,3'-diethyl-2,2'-thiadicarbocyanine (Di-S-C_2(5)) to monitor inside positive or inside negative membrane potentials, respectively. Positive transmembrane potential accelerates the rate of crystallization of Ca^{2+}-ATPase, while negative potential disrupts preformed Ca^{2+}-ATPase crystals, suggesting an influence of transmembrane potential upon the conformation of Ca^{2+}-ATPase.

Measurement of Ca^{2+} translocation by Arsenazo III--loaded Sarcoplasmic Reticulum Vesicles (3)

Release of Ca^{2+} from the $(Ca^{2+} + Mg^{2+})$-ATPase into the interior of intact sarcoplasmic reticulum vesicles was measured using arsenazo III, a metallochromic indicator of Ca^{2+}. Arsenzo III was placed inside the sarcoplasmic reticulum vesicles by making the vesicles transiently leaky with an osmotic gradient in the presence of arsenazo III. External arsenazo III was then removed by centrifugation. Addition of ATP to the $(Ca^{2+} + Mg^{2+})$-ATPase in the presence of Ca^{2+} causes the rapid phophorylation of the enzyme at which time the bound Ca^{2+} becomes inaccessible to external EGTA. The release of Ca^{2+} from the $(Ca^{2+} + Mg^{2+})$-ATPase to the interior of the vesicle measured with intravesiculat arsenazo III was much slower indicating that there is an occluded form of the Ca^{2+}-binding site which precedes the release of Ca^{2+} into the vesicle. The rate of Ca^{2+} accumulation by sarcoplasmic reticulum vesicles is increased by K^+ (5-100mM) and ATP (50-1000 μ M) but the initial rate of Ca^{2+} translocation measured after the simultaneous addition of ATP and EGTA to vesicles that were preincubated in Ca^{2+} was not influenced by these concentrations of K^+ and ATP.

References

1 Beeler, T., Gable, K., and Keffer, J. (1983) Characterization of the Membrane Bound Mg^{2+}-ATPase of Rat Skeletal Muscle. Biochem Biophys Acta 734, 221-234.

2 Beeler, T., Dux, L., and Martonosi, A. (1984) Effect of Na_3VO_4 and Membrane Potential on the Structure of Sarcoplasmic Reticulum Membrane. J. Membrane Biol. 78, 73-79.

3 Beeler, T., and Keffer, J. (1984) THe Rate of Ca^{2+} Translocation by Sarcoplasmic Reticulum $(Ca^{2+}+Mg^{2+})$-ATPase Measured with Intravesicular Arsenazo III. Biochem Biophys Acta 773, 99-105.

Biochimica et Biophysica Acta, 773 (1984) 99–105
Elsevier

BBA 72113

THE RATE OF Ca^{2+} TRANSLOCATION BY SARCOPLASMIC RETICULUM (Ca^{2+} + Mg^{2+})-ATPase MEASURED WITH INTRAVESICULAR ARSENAZO III

TROY BEELER and JEANNE KEFFER

Department of Biochemistry, Uniformed Services University of the Health Sciences, 4301 Jones Bridge Road, Bethesda, MD 20814 (U.S.A.)

(Received December 21st, 1983)

Key words: (Ca^{2+} + Mg^{2+})-ATPase; Ca^{2+} transport; Arsenazo III; Membrane vesicle; Sarcoplasmic reticulum; (Rabbit skeletal muscle)

Release of Ca^{2+} from the (Ca^{2+} + Mg^{2+})-ATPase into the interior of intact sarcoplasmic reticulum vesicles was measured using arsenazo III, a metallochromic indicator of Ca^{2+}. Arsenazo III was placed inside the sarcoplasmic reticulum vesicles by making the vesicles transiently leaky with an osmotic gradient in the presence of arsenazo III. External arsenazo III was then removed by centrifugation. Addition of ATP to the (Ca^{2+} + Mg^{2+})-ATPase in the presence of Ca^{2+} causes the rapid phosphorylation of the enzyme at which time the bound Ca^{2+} becomes inaccessible to external EGTA. The release of Ca^{2+} from the (Ca^{2+} + Mg^{2+})-ATPase to the interior of the vesicle measured with intravesicular arsenazo III was much slower indicating that there is an occluded form of the Ca^{2+}-binding site which precedes the release of Ca^{2+} into the vesicle. The rate of Ca^{2+} accumulation by sarcoplasmic reticulum vesicles is increased by K^+ (5–100 mM) and ATP (50–1000 μM) but the initial rate of Ca^{2+} translocation measured after the simultaneous addition of ATP and EGTA to vesicles that were preincubated in Ca^{2+} was not influenced by these concentrations of K^+ and ATP.

Introduction

Ca^{2+} transport by sarcoplasmic reticulum vesicles is mediated by the (Ca^{2+} + Mg^{2+})-ATPase. The generally accepted mechanism for (Ca^{2+} + Mg^{2+})-ATPase is shown in Scheme I [1–4].

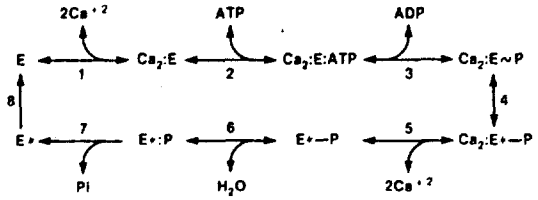

Abbreviation: EGTA, ethyleneglycol bis(β-aminoethyl ether)-*N,N'*-tetraacetic acid.

Following the binding of external Ca^{2+} to the high affinity Ca^{2+}-binding sites on the (Ca^{2+} + Mg^{2+})-ATPase (Step 1), the enzyme is rapidly phosphorylated by ATP (Step 3). The phosphorylation presumably causes a conformational change of the ATPase which alters both the affinity and orientation of the Ca^{2+} binding sites (Step 4). Ca^{2+} is then released into the lumen of the sarcoplasmic reticulum (Step 5) and the phosphoenzyme bond is hydrolyzed (step 6).

Upon phosphorylation, the Ca^{2+} bound to the (Ca^{2+} + Mg^{2+})-ATPase rapidly becomes inaccessible to external EGTA [5–8]. Addition of ADP along with EGTA causes the rapid release of Ca^{2+} due to the reversal of Step 3 [8–10]. Dupont demonstrated that the release of Ca^{2+} by EGTA + ADP was much faster than the relase of Ca^{2+}

from the phosphoenzyme by EGTA + X537A (a Ca^{2+} ionophore) [8]. The former condition causes the reversal of Step 3 while the latter condition depends on the rate at which Ca^{2+} is released from the $(Ca^{2+} + Mg^{2+})$-ATPase into the interior of the sarcoplasmic reticulum vesicle and translocated out of the vesicle by X537A. It is also possible that X537A directly removes Ca^{2+} bound to the protein at a site not exposed to the aqueous phase [11,12].

We have developed a more direct method to measure the rate of Ca^{2+} release from the $(Ca^{2+} + Mg^{2+})$-ATPase into intact vesicles using the Ca^{2+} indicator arsenazo III inside the vesicle. Our results indicate that the release of Ca^{2+} into the interior of the vesicle is relatively slow while the removal of bound Ca^{2+} from the external medium is quite rapid. Therefore the Ca^{2+} must reside in an occluded form during much of the transport cycle.

Methods and Materials

$^{45}CaCl_2$ and [γ-^{32}P]ATP were purchased from New England Nuclear (Boston, MA). All other chemicals were obtained from Sigma (St. Louis, MO).

Methods

Preparation of arsenazo III-loaded sarcoplasmic reticulum vesicles. The microsomal fraction from rabbit skeletal muscle was prepared as previously described [13]. The microsome fraction contains mostly fragmented sarcoplasmic reticulum vesicles. This fraction was then placed on a 30–45% sucrose gradient and centrifuged for 15 h at 4°C at $100\,000 \times g$. The low-density sarcoplasmic reticulum vesicle fraction (32–34%) was removed from the gradient and diluted 1 : 7 into 20 mM arsenazo III/25 mM $MgSO_4$ (pH 6.8). The osmotic imbalance across the membrane of the vesicles causes them to swell [14] allowing the influx of arsenazo III. The free arsenazo III was then removed by collecting the sarcoplasmic reticulum by centrifugation ($100\,000 \times g$ for 30 min.) and resuspending them in arsenazo III-free medium (0.15 M potassium glutamate/10 mM histidine/5 mM $MgSO_4$/0.5 mM EGTA/0.45 mM $CaCl_2$). The centrifugation was repeated four times. The final pellet was resuspended to a protein concentration of 16 mg/ml, frozen in liquid nitrogen, and stored at −70°C.

Phosphorylation of the $(Ca^{2+} + Mg^{2+})$-ATPase by ATP. Ca^{2+} transport was initiated in medium containing 0.1 mM [γ-^{32}P]ATP (1 μCi/ml). At various times the reaction was stopped by the addition of 5% trichloroacetic acid, 0.1 M KH_2PO_4, 5% polyphosphate. The samples were centrifuged at $1000 \times g$ for 20 min. The supernatant was removed and the amount of $^{32}PO_4$ determined by the method described by De Meis and Carvalho [15]. The pellets were washed three times by centrifugation using the trichloroacetic acid solution. The final pellet was resuspended in Lowry C reagent [16] and the amount of ^{32}P in the pellet was determined by measuring the Cerenkov radiation in a scintillation counter. The protein content in each sample was then assayed by the method of Lowry et al. [16].

Results

Our procedure for preparing arsenazo III-loaded sarcoplasmic reticulum vesicles did not differ from the standard way of isolating sarcoplasmic reticulum vesicles except that the vesicles obtained from the sucrose gradient following centrifugation were diluted into an arsenazo III-containing medium. The transient swelling of the sucrose-equilibrated vesicles following dilution in a hypotonic solution made the membrane leaky [14] allowing arsenazo III to enter the vesicles. Following equilibration of the vesicles, the extravesicular arsenazo III was then removed by centrifugation. Neither the

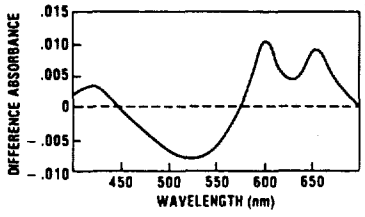

Fig. 1. Difference spectrum of arsenazo III-loaded sarcoplasmic reticulum vesicles following Ca^{2+} uptake. The [illegible] and reference cuvettes contained 0.15 M potassium glutamate, 10 mM histidine, 5 mM $MgSO_4$, 50 μM $CaCl_2$ and arsenazo III-loaded sarcoplasmic reticulum (0.4 mg/ml protein). The spectrum was taken 1 min after the addition of 0.1 mM ATP to the sample cuvette. Temperature = 1°C.

Ca^{2+}-loading capacity (120–150 nmol Ca^{2+}/mg) nor the Ca^{2+}-dependent ATPase activity (0.5–0.8 μmol/mg min) at 25°C was significantly altered by the arsenazo III loading procedure.

Fig. 1 shows the difference spectrum of arsenazo III-loaded vesicles following the addition of ATP in the presence of Ca^{2+}. Under these conditions the vesicles accumulate Ca^{2+}. The spectrum is identical to the difference spectrum obtained when 2.5 mM Ca^{2+} is added to the sarcoplasmic reticulum vesicles in the presence of the Ca^{2+} ionophore, A23187. In the absence of free Ca^{2+}, ATP did not alter the arsenazo III spectrum. Following Ca^{2+} uptake by the sarcoplasmic reticulum vesicles, removal of the free extravesicular Ca^{2+} by EGTA did not have an immediate effect on the arsenazo III spectrum. These experiments demonstrate that arsenazo III was responding only to intravesicular Ca^{2+}.

The use of intravesicular arsenazo III the measure the rate of Ca^{2+} influx is demonstrated in Fig. 2. Ca^{2+} influx at 1°C was initiated by the additionof 2.5 mM Ca^{2+} or the addition of ATP to activate Ca^{2+} transport. The rate of passive Ca^{2+} influx was dependent on the external Ca^{2+} concentration and was increased by the addition of A23187. At 2.5 mM Ca^{2+}, the absorbance change of the intravesicular arsenazo III was not linear. About 17% of the Ca^{2+}-induced absorbance change occurred relatively fast (first order rate constant = 0.23 s^{-1}). This initial phase was

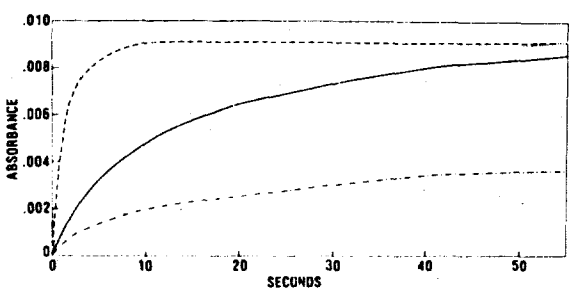

Fig. 2. Absorbance change of arsenazo III-loaded sarcoplasmic reticulum during Ca^{2+} influx. The sample contained 0.1 M potassium glutamate, 10 mM histidine (pH 6.8), 5 mM $MgSO_4$, 50 μM $CaCl_2$ and arsenazo III-loaded vesicles (0.4 mg/ml protein). Ca^{2+} influx was initiated by the addition of 2.5 mM $CaCl_2$ (– – –), 2.5 mM $CaCl_2$ and 2.5 μM A23187 (· · · · · ·), 2.5 mM $CaCl_2$ and 10 μM A23187 (– – –), or 0.1 mM ATP (———). The absorbance change of arsenazo III was monitored at 660 nm using 685 nm as a reference wavelength.

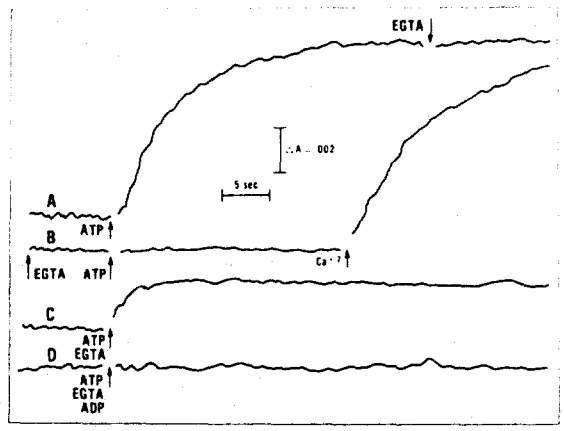

Fig. 3. Effect of EGTA on the absorbance change of arsenazo III-loaded sarcoplasmic reticulum vesicles during Ca^{2+} uptake. The samples contain 0.1 M potassium glutamate, 10 mM histidine, 5 mM $MgSO_4$, 50 μM $CaCl_2$ and arsenazo III-loaded sarcoplasmic reticulum vesicles (0.4 mg/ml protein) at 1°C. At the indicated time, ATP (0.1 mM), EGTA (1 mM), $CaCl_2$ (0.9 mM) or ADP (1 mM) was added. The absorbance change of arsenazo III at 660 nm was monitored using 685 nm as a reference wavelength.

followed by a much slower one in which the absorbance change was less than $3 \cdot 10^{-5}\ \Delta A$/min. The addition of 10 μM A23187 increased the rate of Ca^{2+} influx 300-fold. The rate of Ca^{2+} influx in the presence of 2.5 mM $CaCl_2$ and 2.5 μM A23187 was similar to the rate measured during active Ca^{2+} transport at an external Ca^{2+} concentration of 50 μM.

As stated before, the removal of external Ca^{2+} by EGTA after Ca^{2+} loading does not cause an immediate change in the arsenazo III absorbance (Fig. 3, trace A). But the addition of EGTA to the vesicles before ATP prevents Ca^{2+} uptake and the corresponding absorbance change of arsenazo III (Fig. 3, trace B).

When ATP and EGTA are added at the same time, only the Ca^{2+} initially bound to the (Ca^{2+} + Mg^{2+})-ATPase can be transported (Fig. 3, trace C) [5,7,22–24]. This is demonstrated by the experiment shown in Fig. 4. Ca^{2+} uptake was measured using $^{45}Ca^{2+}$ as a tracer. When the arsenazo III-loaded vesicles were equilibrated with the $^{45}Ca^{2+}$ containing solution, addition of ATP caused a rapid accumulation of about 4 nmol Ca^{2+}/mg protein which was followed by a much slower rate of Ca^{2+} uptake (0.4 nmol/s per mg). The steady-

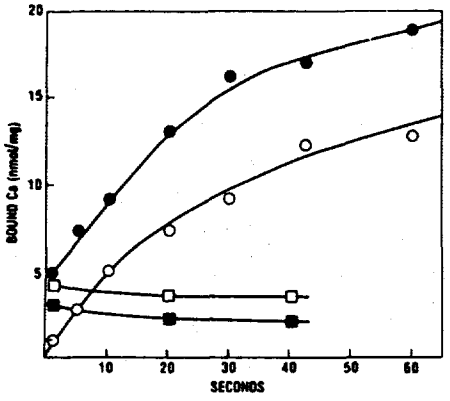

Fig. 4. Ca^{2+} uptake by sarcoplasmic reticulum. The medium contained 0.1 M potassium glutamate, 10 mM histidine (pH 6.8), 5.0 mM $MgSO_4$ 50 μM $^{45}CaCl_2$ (1 μCi/ml), and either arsenazo III-loaded sarcoplasmic reticulum vesicles (0.4 mg/ml protein) (●,□,■) or 0.1 mM ATP (○) at 1°C. Ca^{2+} uptake was initiated by the addition of either 0.1 mM ATP (●,□), 0.1 mM ATP + 1 mM EGTA (■), or sarcoplasmic reticulum vesicles (0.4 mg/ml protein) (○) preincubated in potassium glutamate medium without ^{45}Ca. To one of the samples (□), 1 mM EGTA was added 1 s after the ATP addition. At various times, the samples were diluted 1 : 10 with 0.1 M potassium glutamate, 10 mM histidine (pH 6.8), 5 mM $MgSO_4$ and 1 mM EGTA and passed through Millipore HA filters. The filters were immediately washed with 2 ml of EGTA wash solution. After drying the filters, the amount of $^{45}Ca^{2+}$ bound to the filters was measured in a scintillation counter using a nonaqueous counting solution.

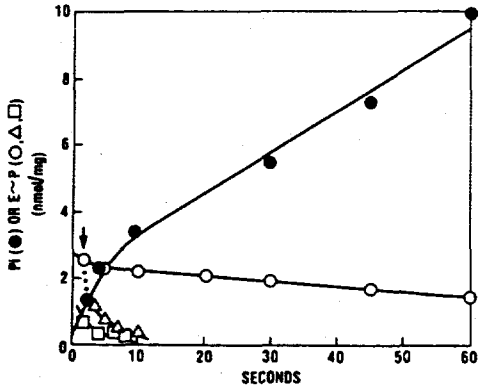

Fig. 5. Formation of the phosphorylated enzyme intermediate and the release of inorganic phosphate by the $(Ca^{2+} + Mg^{2+})$-ATPase during Ca^{2+} transport. The medium contained 0.1 M potassium glutamate, 10 mM histidine (pH 6.8), 5 mM $MgSO_4$, 0.1 mM [γ-^{32}P]ATP (1 μCi/ml), and either 50 μM $CaCl_2$ (△,●,○) or 1.0 mM EGTA (□). Ca^{2+} transport was initiated by the addition of sarcoplasmic reticulum vesicles (0.4 mg/ml) which were equilibrated in potassium glutamate solution containing 50 μM $CaCl_2$. To one sample, 1 mM EGTA was added to the medium 2 s after the reaction was initiated (△). All values represent the Ca^{2+}-dependent E ~ P formation or Ca^{2+}-dependent release since the background obtained from experiments in which the vesicles and media contained 1 mM EGTA was subtacted from the data obtained when the medium and/or the vesicles contained Ca^{2+}.

state level of the phosphorylated intermediate of these vesicles was about 2.5 nmol E-P/mg protein (Fig. 5). Even when EGTA was added together with ATP there was a rapid uptake of about 3 nmol Ca^{2+}/mg but no subsequent accumulation since the free Ca^{2+} was chelated by EGTA. When Ca^{2+} transport was initiated by the simultaneous addition of ATP and $^{45}Ca^{2+}$ to vesicles equilibrated in the absence of ^{45}Ca, there was no burst of $^{45}Ca^{2+}$ uptake since only the unlabeled bound Ca^{2+} was carried by the first turnover. The appearance of the bound Ca^{2+} in the interior of sarcoplasmic reticulum vesicle following ATP addition as detected by intravesicular arsenazo III was much slower (first order rate = 0.45 s^{-1}) (Fig. 3, trace C) than the rate at which it becomes inaccessible to external EGTA. The rate of Ca^{2+} release into the interior of the vesicle was comparable to the rate at which the phosphoenzyme intermediate decomposes (Fig. 5).

When 1 mM ADP was added along with ATP and EGTA, neither Ca^{2+} translocation (Fig. 3, trace D) nor $^{45}Ca^{2+}$ uptake (data not shown) [9,10] was observed. Since ADP accelerates the reversal of Step 3 of Scheme I it is likely that in the presence of ADP the rate of Ca^{2+} release by the reversal of steps 1–4 or steps 1–3 is much faster than Ca^{2+} translocation (steps 3–5).

The $(Ca^{2+} + Mg^{2+})$-ATPase is activated by K^+ [25–31] and high concentrations of ATP [32–35]. The initial rate of absorbance change of arsenazo III-loaded vesicles during Ca^{2+} uptake at 1°C increased from $5.1 \cdot 10^{-4}\ \Delta A/s$ in the presence of 2 mM K^+ to $11 \cdot 10^{-4}\ \Delta A/s$ in the presence of 100 mM K^+ (Fig. 6). Increasing the ATP concentration from 50 μM to 1.0 mM increased the initial rate of absorbance change from $9.5 \cdot 10^{-4}\ \Delta A/s$ to $21 \cdot 10^{-4}\ \Delta A/s$ (Fig. 7A). Since the K_m of the Ca^{2+}-ATPase for ATP is about 3 μM [9],

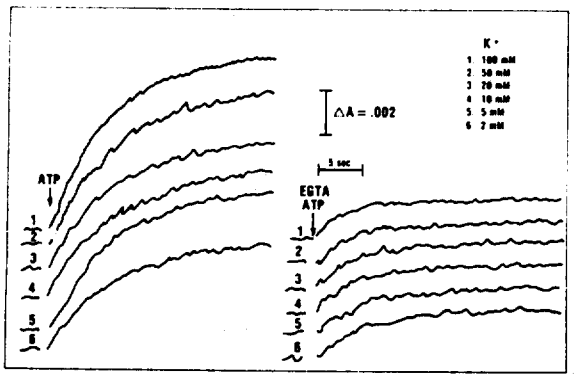

Fig. 6. Effect of K^+ on the rate of Ca^{2+} translocation by sarcoplasmic reticulum. The medium contained 10 mM histidine (pH 6.8), 5.0 mM $MgSO_4$, 50 μM $CaCl_2$, arsenazo III-loaded sarcoplasmic reticulum vesicles (0.4 mg/ml) and varying ratios of 0.2 M glycine and 0.1 M potassium glutamate. Ca^{2+} uptake was initiated by the addition of 0.1 mM ATP (left) or 0.1 mM ATP + 1 mM EGTA (right). The absorbance change at 660 nm was monitored in an Aminco DW-2 spectrophotometer in the dual wavelength mode using 685 nm as the reference wavelength.

most of this increase in the uptake rate is attributed to an activation of an intermediate step in the reaction cycle. When Ca^{2+} transport was initiated by the simultaneous addition of ATP and EGTA there was no effect of high concentrations of ATP (0.1–1.0 mM) (Fig. 7B) or K^+ (Fig. 6) on the appearance of Ca^{2+} inside the vesicles. This data suggests that K^+ and ATP activate an intermediate reaction which follows the release of Ca^{2+} into the vesicle.

It was previously demonstrated that Ca^{2+} transport is activated by inside negative membrane potentials generated by K^+ gradients in the presence of the K^+ ionophore valinomycin [36–38]. In order to measure the effect of K^+ gradients on the rate of Ca^{2+} transport at 1°C, arsenazo III-loaded vesicles equilibrated in potassium glutamate were diluted 50-fold into either glycine or potassium glutamate medium containing valinomycin. When Ca^{2+} transport was initiated at the time of the dilution, the rate of Ca^{2+} uptake in the glycine and potassium glutamate solutions monitored by both the absorbance change of the intravesicular

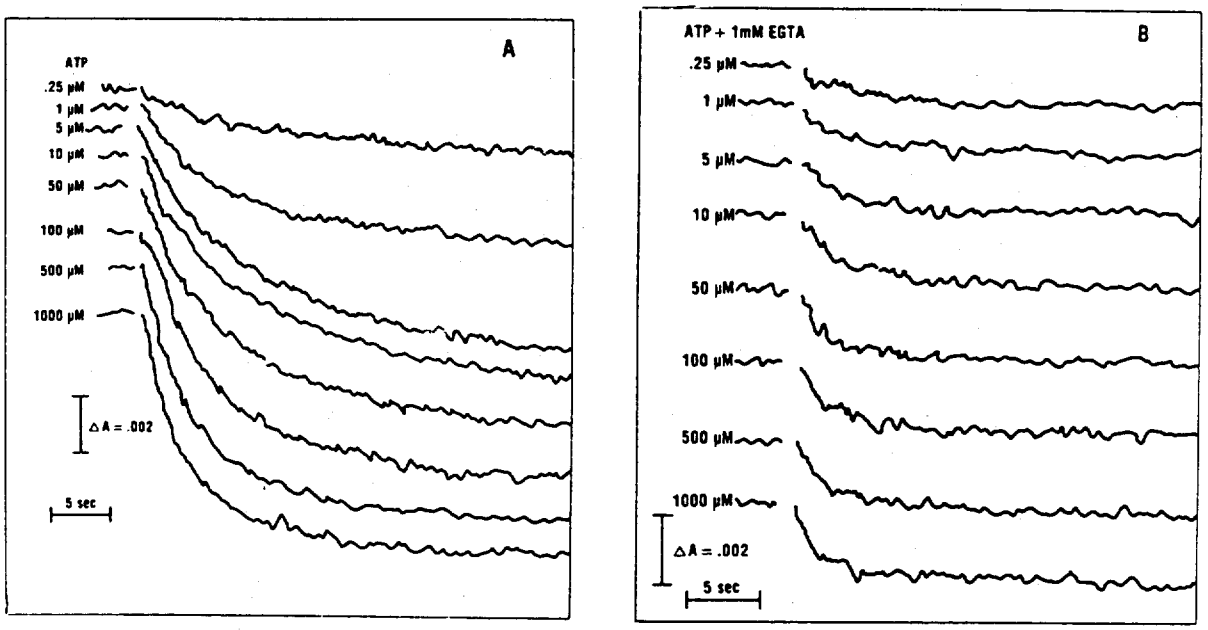

Fig. 7. Effect of ATP on the initial rate of Ca^{2+} translocation into sarcoplasmic reticulum vesicles. The medium contained 0.1 M potassium glutamate, 10 mM histidine (pH 6.8), 5 mM $MgSO_4$, 50 μM $CaCl_2$, and arsenazo III-loaded sarcoplasmic vesicles (0.4 mg/ml). Ca^{2+} transport was initiated by the addition of varying amounts of ATP with (Panel B) or without (Panel A) 1 mM EGTA. The absorbance change of arsenazo III at 660 nm was monitored in an Aminco DW-2 spectrophotometer in the dual wavelength mode using 685 nm as a reference wavelength. An increase in the asorbance at 660 nm is indicated by downward trace.

arsenazo III (as in Fig. 6) or by the accumulation of $^{45}Ca^{2+}$ (as in Fig. 5) was essentially the same. Allowing the vesicles to equilibrate in the dilution medium before the initiation of Ca^{2+} transport gives the same results as shown in Fig. 6. Under these conditions (1°C) the activation of Ca^{2+} transport by K^+ is the same whether the K^+ is on both sides of the membrane or just on the internal side. At 15°C, the rate of Ca^{2+} accumulation of K^+-equilibrated vesicles was much greater in glycine (+valinomycin) than in potassium glutamate (+valinomycin) medium [37].

The rate of Ca^{2+} translocation measured by the absorbance change of arsenazo III-loaded sarcoplasmic reticulum vesicles equilibrated in potassium glutamate medium following a 50-fold dilution into glycine medium containing ATP, EGTA and valinomycin did not significantly differ from that observed after diluting into potassium glutamate medium containing ATP and EGTA. These experiments along with the one in Fig. 6 indicate that the rate of the initial Ca^{2+} translocation by vesicle equilibrated in K^+ medium is the same in glycine medium as that in potassium glutamate even when a K^+ gradient (and therefore a membrane potential [37–39]) is present.

Discussion

A technique was developed to prepare sarcoplasmic reticulum vesicles loaded with arsenazo III. Other optical probes such as chlortetracycline [40,41] and 8-anilino-1-naphthalenesulfonate [12,42–44] can measure internal Ca^{2+} but they lack specificity and have slow response times. The response time of arsenazo III is quite rapid (Ca^{2+} on an off time = 2–5 ms) [45,46] and the change in the absorbance spectrum of arsenazo III due to Ca^{2+} is very different than that caused by changes in the Mg^{2+} or H^+ concentration. Because the affinity of arsenazo III for Ca^{2+} is so high and the amount of dye that is trapped by the vesicles ($\cong$ 3 nmol/mg protein) was well below the capacity of the vesicles to accumulate Ca^{2+}, the intravesicular arsenazo III rapidly became saturated with Ca^{2+} after initiation of Ca^{2+} transport. This makes quantitation of the amount of Ca^{2+} translocated difficult. A Ca^{2+} indication of much lower affinity would be more useful in measuring the intravesicular Ca^{2+} concentration during Ca^{2+} accumulation. Using the same loading technique we were unable to prepare vesicles with the Ca^{2+} indicators, murexide or antipyrylazo III, due to problems with solubility of the probes and damage to the vesicles.

The appearance of Ca^{2+} within the vesicle upon the initiation of Ca^{2+} transport was much slower than its removal from the external medium. This provides direct evidence for an occluded state during Ca^{2+} uptake [8,24,47]. Ikemoto [48] measured the rate of Ca^{2+} release from isolated (Ca^{2+} + Mg^{2+})-ATPase following phosphorylation with 5 μM ATP at 22°C. This preparation did not accumulate Ca^{2+} due to the leakiness of the membrane following Triton X-100 treatment. Ca^{2+} release followed E-P formation with a lag time of 15 ms. At this low ATP concentration, the maximum phosphorylation level (0.1 mol E-P/mol ATPase) was reached within 150 ms after ATP addition while the maximum level of Ca^{2+} release (0.24 mol Ca^{2+}/mol ATPase) was reached after 250 ms. The work presented here confirms that with intact vesicles, there is a lag time between phosphorylation and Ca^{2+} release from the (Ca^{2+} + Mg^{2+})-ATPase.

Although the rate of Ca^{2+} transport is increased by K^+ (10–100 mM) and by ATP (50–1000 μM), the initial rate of Ca^{2+} translocation was not influenced by K^+ or high ATP concentrations. The most likely explanation is that K^+ and ATP activates an intermediate reaction which follows the release of Ca^{2+} from the (Ca^{2+} + Mg^{2+})-ATPase into the interior of the vesicle.

Acknowledgements

This work was supported by research grants from the National Institutes of Health (GM 29300), from the Office of Naval Research and by the Uniformed Services University of the Health Sciences.

References

1 Martonosi, A. and Beeler, T.J. (1983) in Handbook of Physiology (Peachey, L.D. and Adrian, R.H., eds.), Vol 10, pp. 417–485, Waverly Press, Baltimore, MD
2 Yamamoto, T., Takisawa, H. and Tonomura, Y. (1979) Curr. Top. Bioenerg. 9, 179–236

3 Hasselbach, W. (1979) Top. Curr. Chem. 78, 1–56
4 Ikemoto, N. (1982) Annu. Rev. Physiol. 44, 297–317
5 Verjovski-Almeida, S., Kurzmack, M. and Inesi, G. (1978) Biochemistry 17, 5006–5013
6 Sumida, M. and Tonomura, Y. (1974) J. Biochem. (Tokyo) 75, 283–297
7 Ikemoto, N., Garcia, A.M., Kurobe, Y. and Scott, T.L. (1981) J. Biol. Chem. 256, 8593–8601
8 Dupont, Y. (1980) Eur. J. Biochem. 109, 231–238
9 Kanazawa, T., Yamada, S., Yamamoto, T. and Tonomura, Y. (1971) J. Biochem. (Tokyo) 70, 95–123
10 Makinose, M. and Hasselbach, W. (1977) FEBS Lett. 12, 271–272
11 Diamond, E., Norton, K.B., McIntosh, D. and Berman, M. (1980) J. Biol. Chem. 255, 11351–11356
12 Pick, U. and Racker, E. (1979) Biochemistry 18, 2608–2613
13 Duggan, P.F. and Martonosi, A. (1970) J. Gen. Physiol. 56, 147–167
14 Meissner, G. and McKinely, D. (1976) J. Membrane Biol. 30, 79–98
15 De Meis, L. and Carvalho, M.C. (1974) Biochemistry 13, 5032–5038
16 Lowry, O.H., Rosebrough, N.J., Farr, A.L. and Randall, R.J. (1951) J. Biol. Chem. 193, 265–275
17 Rauch, B., Gahk, D. and Hasselbach, W. (1978) FEBS Lett. 93, 65–68
18 Sumida, M., Wang, M.T., Mandel, F. Froehlich, J.P. Schwartz, A. (1978) J. Biol. Chem. 253, 8772–8777
19 Guillain, F., Gingold, M., Buschlen, S. and Champeil, P. (1980) J. Biol. Chem. 255, 2072–2076
20 McIntosh, D. and Berman, M.C. (1978) J. Biol. Chem. 253, 5140–5146
21 Chiu, V.C. and Haynes, D.H. (1980) J. Membrane Biol. 56, 219–239
22 Kurzmack, M., Verjovski-Almeida, S. and Inesi, G. (1977) Biochem. Biophys. Res. Commun. 78, 772–776
23 Chiesi, M. and Inesi, G. (1979) J. Biol. Chem. 254, 10370–10377
24 Takakuwa, Y. and Kanazawa, T. (1979) Biochem. Biophys. Commun. 88, 1209–1216
25 Duggan, P.F. (1977) J. Biol. Chem. 252, 1620–1627
26 Katz, A.M. and Repke, D.I. (1967) Circ. Res. 21, 767–775
27 Yamada, S.T., Yamamoto, T. and Tonomura, Y. (1970) J. Biochem. (Tokyo) 67, 789–794
28 Shigekawa, M. and Pearl, L.J. (1976) J. Biol. Chem. 251, 6947–6952
29 Shigekawa, M. and Dougherty, J.P. (1978) J. Biol. Chem. 253, 1451–1457
30 Shigekawa, M. and Dougherty, J.P. (1978) J. Biol. Chem. 253, 1458–1464
31 Shigekawa, M., Dougherty, J.P. and Katz, A.M. (1978) J. Biol. Chem. 253, 1442–1450
32 De Meis, L. and De Mello, M.C. (1973) J. Biol. Chem. 248, 3691–3701
33 Froehlich, J.P. and Taylor, E.W. (1975) J. biol. Chem. 250, 2013–2021
34 Verjovski-Almeida, S. and Inesi, G. (1979) J. Biol. Chem. 254, 18–21
35 Yamamoto, T. and Tonomura, Y. (1967) J. Biochem. (Tokyo) 62, 558–575
36 Zimmak, P. and Racker, E. (1978) J. Biol. Chem. 253, 4631–4637
37 Beeler, T.J. (1980) J. Biol. Chem. 255, 9156–9161
38 Beeler, T.J., Farmen, R.H. and Martonosi, A.N. (1981) J. Membrane Biol. 62, 113–137
39 Beeler, T.J., Russell, J.T. and Martonosi, A.N. (1979) Eur. J. Biochem. 95, 579–591
40 Caswell, A.H. (1972) J. Membrane Biol. 7, 345–364
41 Millman, M.S., Caswell, A. and Haynes, D. (1980) Membrane Biochem. 3, 291—1315
42 Chiu, V.C.K., Mourning, D., Watson, B.D. and Haynes, D. (1980) J. Membrane Biol. 56, 121–132
43 Vanderkooi, J.M. and Martonosi, A. (1971) Arch. Biochem. Biophys. 144, 87–98
44 Vanderkooi, J.M. and Martonosi, A. (1971) Arch. Biochem. Biophys. 144, 99–106
45 Scarpa, A., Brinley, F.J., Tiffert, T. and Dubyak, G.R. (1978) Ann. NY Acad. Sci. 307, 86–111
46 Scarpa, A. (1979) Methods Enzymol. 56, 301–338
47 Takisawa, H. and Makinose, M. (1981) Nature 290, 270–273
48 Ikemoto, N. (1976) J. Biol. Chem. 251, 7272–7277

Biochimica et Biophysica Acta, 734 (1983) 221–234
Elsevier

BBA 71832

CHARACTERIZATION OF THE MEMBRANE BOUND Mg^{2+}-ATPase OF RAT SKELETAL MUSCLE

TROY J. BEELER, KENNETH S. GABLE and JEANNE M. KEFFER

Department of Biochemistry, Uniformed Services University of the Health Sciences, 4301 Jones Bridge Road, Bethesda, MD 20814 (U.S.A.)

(Received May 17th, 1983)

Key words: Mg^{2+}-ATPase; Membrane integrity; (Rat skeletal muscle)

A procedure was developed to isolate a membrane fraction of rat skeletal muscle which contains a highly active Mg^{2+}-ATPase (5–25 μmol P_i/mg min). The rate of ATP hydrolysis by the Mg^{2+}-ATPase was nonlinear but decayed exponentially (first-order rate constant $\geq 0.2\ s^{-1}$ at 37°C). The rapid decline in the ATPase activity depended on the presence of ATP or its nonhydrolyzable analog 5'-adenylyl imidodiphosphate (Ado*PP*[NH]*P*). Once inactivated, removal of ATP from the medium did not immediately restore the original activity. ATP- or Ado*PP*[NH]*P*-dependent inactivation could be blocked by concanavalin A, wheat germ agglutinin or rabbit antiserum against the membrane. Additions of these proteins after ATP addition prevented further inactivation but did not restore the original activity. Low concentrations of ionic and nonionic detergents increased the rate of ATP-dependent inactivation. Higher concentrations of detergents, which solubilize the membrane completely, inactivated the Mg^{2+}-ATPase. Cross-linking the membrane components with glutaraldehyde prevented ATP-dependent inactivation and decreased the sensitivity of the Mg^{2+}-ATPase to detergents. It is proposed that the regulation of the Mg^{2+}-ATPase by ATP requires the mobility of proteins within the membrane. Cross-linking the membrane proteins with lectins, antiserum or glutaraldehyde prevents inactivation; increasing the mobility with detergents accelerates ATP-dependent inactivation.

Introduction

The microsomal subcellular fraction of skeletal muscle contains both a Ca^{2+}-dependent ATPase and a Ca^{2+}-independent Mg^{2+}-ATPase. The Ca^{2+}-ATPase mediates the active transport of Ca^{2+} into the sarcoplasmic reticulum. The function of the Mg^{2+}-ATPase has not been identified. Fernandez et al. [1] demonstrated that vesicles containing the Mg^{2+}-ATPase from rabbit skeletal muscle can be separated from sarcoplasmic reticulum vesicles by first selectively loading the sarcoplasmic reticulum with calcium phosphate to increase their density and then fractionating the microsomes by sucrose density centrifugation. The Mg^{2+}-ATPase was associated with those vesicles which migrated to a density between 1.09 and 1.13 g/ml. There are various other reports in the literature on the preparation of a low density subfraction of skeletal muscle microsomes which have high Mg^{2+}-ATPase activity [2–6]. Antibodies specific to the low density vesicle fraction prepared from rabbit skeletal muscle were shown to bind in the region of the transverse tubule [4].

Abbreviations: ADA, *N*-(2-acetamido)-2-iminodiacetic acid; Mops, 3-(*N*-morpholino)propanesulfonic acid; EDTA, ethylenediaminetetraacetic acid; EGTA, ethylene glycol bis(β-aminoethyl ether)-*N*,*N*'-tetraacetic acid; PMSF, phenylmethylsulfonyl fluoride; CCCP, carbonyl cyanide *m*-chlorophenylhydrazone; FCCP, carbonyl cyanide *p*-trifluoromethoxyphenylhydrazone; Ado*PP*[NH]*P*, 5'-adenylyl imidodiphosphate; Chaps, 3-[(3-cholamidopropyl)dimethylammonio]propanesulfonate; Chapso, 3-[(3-cholamidopropyl)dimethylammonio]-2-hydroxy-1-propanesulfonate.

Malouf and Meissner [5] used cytochemical techniques to demonstrate a highly active Mg^{2+}-ATPase in the plasmalemma and transverse tubule of chicken pectoralis muscle.

The purpose of the studies reported here is to investigate the effect of perturbation of the membrane by detergents, lectins, antiserum and glutaraldehyde on the Mg^{2+}-ATPase. Investigations on the regulation of the Mg^{2+}-ATPase may lead to a better understanding of its function.

Materials

Adenosine 5'-triphosphate, 5'-adenylyl imidodiphosphate (Ado*PP*[NH]*P*), lactate dehydrogenase, pyruvate kinase, wheat germ agglutinin, concanavalin A, *N*-ethylmaleimide, 5,5'-dithiobis (2-nitrobenzoic acid), cytocholasin B, vinblastine, colchicine, phenylmethylsulfonylfluoride (PMSF), quercetin, sodium azide, sodium arsenate, *N*-acetylglucosamine, α-methyl mannoside, oligomycin, gramacidin, valinomycin, carbonyl cyanide *p*-trifluoromethoxyphenylhydrazone (FCCP), carbonyl cyanide *m*-chlorophenylhydrazone (CCCP), 2,4-dinitrophenol, soybean lectin (*Glycine max*), lectin from *Bandeiraea simplicifolia*, Triton X-100, polyoxyethylene 20 oleoyl ether (Brij 9)), polyoxyethylene 10 stearyl ether (Brij 76), polyoxyethylene 23 lauryl ether (Brij 35), polyoxyethylene sorbitan monolaurate (Tween 20), polyoxyethylene sorbitan monopalmitate (Tween 40), polyoxyethylene sorbitan monostearate (Tween 60), polyoxyethylene sorbitan monooleate (Tween 80), sodium cholate, sodium deoxycholate, digitonin, phospholipase C, and cholesterol were obtainted from Sigma Chemical Company (St. Louis, MO). Zwittergent 3-8, Zwittergent 3-10, Zwittergent 3-12, Zwittergent 3-14, Zwittergent 3-16, monensin and A23187 were purchased from Calbiochem-Behring Corp. (La Jolla, CA). (γ-^{32}P)labeled adenosine 5'-triphosphate was provided by New England Nuclear (Boston, MA). Ruthenium Red was purchased from Aldrich Chemical Corp. (Milwaukee, WI). Lectins from *Limulus polythemus*, *Pisum sativum* and *Arachis hypogaea* were obtained from E-Y Laboratories (San Mateo, CA). Pierce Chemical Corp. (Rockford, IL) supplied the Chapso, Chaps, 7-chloro-4-nitrobenzo-2-oxa-1,3-diazole (NBD chloride), dansyl chloride, dimethyl adipimidate, dimethyl pimelimidate, dimethyl-3,3'-dithiobis(propionimidate), 2-iminothiolane, disuccinimidyl suberate, disuccinimidyl tartarate, ethylene glycol bis(succinimidyl succinate) and 4,4'-difluoro-3,3'dinitrophenylsulfone.

Methods

Preparation of muscle subcellular fractions

The back and hind leg muscles were removed from 300 g male Sprague-Dawley rats and trimmed of red muscle, connective and adipose tissue. After chopping the muscle into small pieces (about 0.25 cm^3), it was homogenized with a Polytron at low speed for 2 min in 0.15 M KCl, 10 mM *N*-(2-acetamido)-2-iminodiacetic acid (ADA), 10 mM 3-(*N*-morpholino)propanesulfonic acid (MOPS) (pH 6.8), and 5 mM $MgSO_4$ (KCl solution). Every 15 s the Polytron was stopped and the blade cleared of connective tissue. The homogenization and all subsequent steps were perfcrmed at 4°C. The muscle was further homogenized in a 50 ml Potter-Elvehjem homogenizer (five strokes) and then centrifuged at $1500 \times g$ for 10 min. The pellet was saved to prepare the crude myofibril fraction. The supernatant was further centrifuged at $10000 \times g$ for 15 min. The pellet was saved to prepare the crude mitochondrial fraction and the supernatant was centrifuged at $53000 \times g$ for 1 h to collect the microsomal fraction. The supernatant was saved to prepare the cytosol fraction. The microsomal pellet was resuspended in KCl solution and applied to a discontinuous sucrose gradient containing 10% (2 ml), 27% (9 ml), 30% (6 ml), 35% (6 ml), 40% (6 ml) and 45% (3 ml) sucrose made in KCl solution. The microsomes were fractionated by centrifugation at $130000 \times g$ for 3 h. The Mg^{2+}-ATPase containing vesicles were obtained at the 10–27% interphase (low density vesicles). The sarcoplasmic reticulum vesicles were removed from the lower part of the gradient (33–37% sucrose). The low density vesicles were diluted 10-fold in KCl solution and concentrated by centrifugation at $140000 \times g$ for 30 min. The vesicles were placed on another discontinuous sucrose gradient (6 ml 10% sucrose, 6 ml 27% sucrose made in KCl solution) and centrifuged 15 h at $130000 \times g$. The low density vesicles containing the Mg^{2+}-ATPase were removed from the 10–27% interphase.

The crude myofibril fraction was prepared from the 1500 × *g* pellet by rehomogenizing the pellet in 10 volumes of KCl with the Polytron at medium speed. The suspension was then centrifuged 1500 × *g* for 10 min. The pellet was kept as the crude myofibril fraction.

The crude mitochondrial fraction was prepared from the first 10 000 × *g* pellet by resuspending the pellet in 250 ml of KCl solution and centrifuging the suspension at 1500 × *g* for 10 min. The supernatant was centrifuged again at 10 000 × *g* for 15 min. The pellet was resuspended in 250 ml of KCl and the two centrifugations were repeated. The final pellet was used as the crude mitochondrial fraction.

The cytosol fraction was obtained from the 53 000 × *g* supernatant. The supernatant was centrifuged 100 000 × *g* for 30 min and then dialyzed 24 h against KCl solution.

Assays

ATPase activity was measured using a coupled enzyme assay [7] or by monitoring the release of P_i from [γ-^{32}P]ATP [8]. Cholesterol was measured by the method of Courchaine et al. [9], following extraction of membrane lipids as described by Bligh and Dyer [10]. Total phospholipid was determined by measuring the amount of P_i released following the digestion of the lipids by the method of Bartlett [11]. Aldolase [12], pyruvate kinase [13], lactate dehydrogenase [14], and creatine phosphokinase [15] were assayed as previously described, except the assay medium was made in KCl solution. 5'-Nucleotidase was assayed by the method of Dixon and Purdam [16].

SDS-polyacrylamide gel electrophoresis

Polyacrylamide gel electrophoresis was performed following the method of Laemmli [17] using 6–12% acrylamide gradient gels. Gels were stained with 0.2% Coomassie brilliant blue R-125 in 40% methanol, 7% acetic acid and destained with 20% methanol, 7% acetic acid.

The binding of antibodies and lectins to the proteins separated by SDS-polyacrylamide electrophoresis was investigated by first transferring the proteins electrophoretically from the gel to a nitrocellulose sheet in 25 mM Tris-HCl (pH 8.3), 20% methanol at 60 V (about 200 mA) using a Bio-Rad Trans-Blot cell. The nitrocellulose sheet was incubated for 1 h with 1% bovine serum albumin in 10 mM phosphate buffered saline (pH 7.4) to block the remaining protein binding sites of the nitrocellulose sheet. To detect lectin binding sites, peroxidase conjugated lectins (100 ml, 1 μg/ml proteins) were incubated with the nitrocellulose for 2.5 h. The unbound lectin was removed by washing the nitrocellulose sheet five times with 30 ml of phosphate buffered saline containing 0.05% Tween 20. Bound lectin was localized by staining for peroxidase activity using 4-chloro-1-naphthol as described by Hawkes et al. [18]. After staining, the nitrocellulose sheets were washed with excess water.

Antibody binding was detected by first incubating the blocked nitrocellulose sheet with antiserum (or control serum) diluted 1 to 150 in phosphate buffered saline containing 0.01% bovine serum albumin for 3.5 h at room temperature. After the nitrocellulose was then washed three times with phosphate buffer saline, it was incubated with peroxidase conjugated goat antibody to rabbit IgG (0.3 μg/ml protein) in phosphate buffered saline containing 0.01% bovine serum albumin. After incubating 1 h at 25°C, the nitrocellulose sheet was washed and stained with 4-chloro-1-naphthol as described above.

Preparation of rabbit antiserum against the low-density vesicles

Before immunization, serum was collected from the rabbit to serve as control serum. Low density vesicles (1 mg protein emulsified with equal volume of Freund's complete adjuvant) were injected subcutaneously into the back of the rabbit. The injections were repeated after 2 and 4 weeks. Eleven days after the last injection, serum was collected from the rabbit and stored at −20°C.

Electron microscopy

Low density vesicles (0.25 mg of protein) were diluted into 0.1 M cacodylate buffer (pH 7.2) and centrifuged 30 min at 120 000 × *g*. The pellet was fixed for 1 h at 4°C with 2.5% glutaraldehyde in 0.1 M cacodylate buffer containing 1% tannic acid. The fixed pellet was then rinsed with 0.1 M cacodylate and then treated with 2% OsO_4 in 0.1 M cacodylate buffer. After embedding in araldite, the pellet was sectioned and then stained with uranyi acetate and lead citrate.

Results

The highest specific activity of the detergent-sensitive, Ca^{2+}-independent Mg^{2+}-ATPase of rat skeletal muscle was found in the microsomal fraction (Table I). Low-density vesicles in the microsomal fraction which contained the Mg^{2+}-ATPase were separated from the sarcoplasmic reticulum vesicles by sucrose density centrifugation (Table I and Fig. 1). Following a second sucrose density centrifugation (Fig. 1), no detectable Ca^{2+}-dependent ATPase activity remained in the low-density vesicle fraction. The specific activity of the Mg^{2+}-ATPase of the low density vesicles was 26-times larger than that of the sarcoplasmic reticulum. The low density vesicles contained a much higher content of cholesterol (0.6 μmol/mg protein) and 5'-nucleotidase (16 nmol/mg per min) than the microsomal fraction (0.1 μmol/mg and 0.2 nmol/mg per min, respectively) indicating that the plasma membrane and/or the transverse tubule membrane is also enriched in the low-density vesicle fraction.

Analysis of the protein composition of the low-density vesicles by sodium dodecyl sulfate polyacrylamide electrophoresis showed a pattern quite distinct from that of the myofibril, mitochondrial,

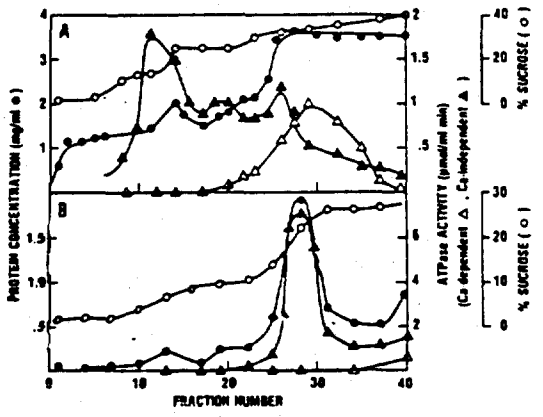

Fig. 1. Separation of microsomal vesicles from rat skeletal muscle. (A) First sucrose gradient. Microsomes (7 ml, 10 mg/ml protein) were placed on a discontinuous sucrose gradient (9 ml 27%, 6 ml 30%, 6 ml 40%, and 3 ml 45% sucrose in KCl medium). After centrifugation for 3 h at 130000 × g, the gradient was fractionated into 0.9-ml aliquots and the protein, Ca^{2+}-dependent and Ca^{2+}-independent activity were measured as described in Methods. (B) Second sucrose gradient. Fraction 9–16 of the first sucrose gradient were pooled diluted with KCl medium and concentrated by centrifugation (140000 × g for 0.5 h). The pellet was resuspended in KCl medium and applied to another discontinuous sucrose gradient (6 ml 10% sucrose, 6 ml 27% sucrose in KCl medium). After centrifugation at 130000 × g for 15 h, the gradient was fractionated into 0.4-ml aliquots and the protein, Ca^{2+}-independent and Ca^{2+}-dependent ATPase activity of each fraction were measured.

TABLE I

Mg^{2+}-ATPase ACTIVITY OF MUSCLE SUBCELLULAR FRACTIONS

Mg^{2+}-ATPase was assayed in medium containing 0.15 M KCl, 10 mM Mops, 5 mM $MgSO_4$, 16 U/ml pyruvate kinase, 5 U/ml lactate dehydrogenase, 0.5 mM phospho*enol*pyruvate, 0.15 mM NADH and 1 mM EGTA. The ATPase activity was determined from the initial rate NADH oxidation as monitored spectrophotometrically at 340 nm. Inhibition by Triton X-100 was measured by including 0.1% Triton X-100 in the assay medium.

Fraction	Initial Mg^{2+}-ATPase activity (μmol/mg min)	
	− Detergent	+0.1% Triton
1 Crude myofibril	0.19	0.19
2 Cytosol	0.03	0.006
3 Crude mitochondria	0.14	0.04
4 Microsome	0.25	0.007
5 Low-density vesicles	6.11	0.11

sarcoplasmic reticulum or cytosol fraction (Fig. 2A). The major unique protein band enriched in the low density vesicle fraction had an apparent molecular weight of about 56000. When separated by isoelectric focusing, this band breaks up into a series of 5 spots with p*I* values ranging from 5.4 to 6 (Fig. 2B). Many of the proteins found in the low-density vesicles appear to be simply trapped inside the vesicles during their preparation. The protein with an apparent M_w of 69000 and a p*I* of 5.8–6.0 had the same migration pattern as authentic rat serum albumin (Fig. 2B). Rosemblatt et al. [4] identified serum albumin as a major protein component in low-density vesicles isolated from rabbit skeletal muscle. The protein with an apparent M_w of 40000 and a p*I* of 6.7–6.9 gave the same migration pattern as authentic creatine phosphokinase. The activity of several soluble cytoplasmic enzymes in the low-density fraction showed a 6–10-fold increase in activity upon addi-

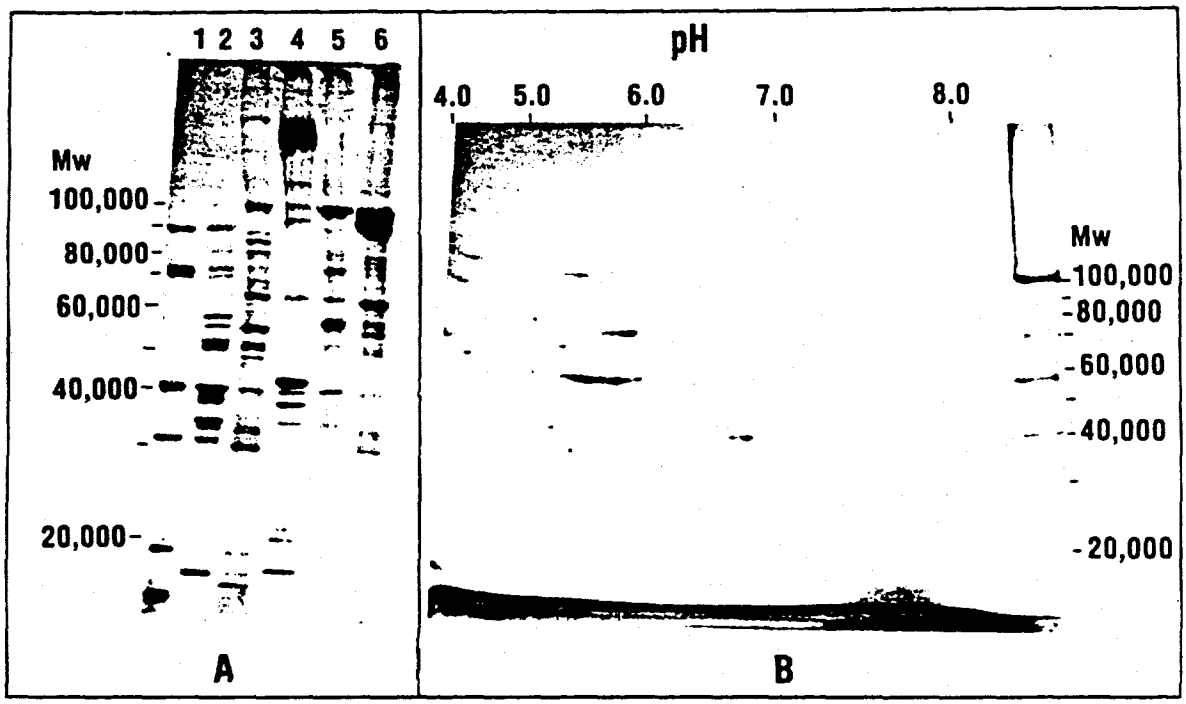

Fig. 2. Comparison of the protein composition of the low-density vesicle fraction with other subcellular fractions by SDS-polyacrylamide electrophoresis. (A) SDS-polyacrylamide gel electrophoresis was performed by the method described by Laemmli [17] using 6–12% acrylamide gradient gels. Each sample except the molecular weight standards (10 μg proteins) (phosphorylase *b*, bovine serum albumin, ovalbumin, carbonic anhydrase, soybean trypsin inhibitor and α-lactalbumin); lane 2, cytosol; lane 3, mitochondrial fraction; lane 4, myofibril fraction; lane 5, low density vesicles and lane 6, sarcoplasmic reticulum. (B) Two-dimensional electrophoresis of the low-density fraction. Procedure of O'Farrell [25] was followed. Low-density vesicles (200 μg protein were solubilized in 10% Triton X-100 for the first dimension, isoelectric focusing electrophoresis. A 6–12% acrylamide gradient gel was used for the second dimension. SDS polyacrylamide gel electrophoresis.

tion of 0.1% Triton X-100 (Table II). The latent, specific activity of these enzymes in the low-density vesicle fraction was 1/6 to 1/25 of the specific activity of these enzymes in the cytosol fraction indicating that up to 16% of the protein found in the low-density fraction may simply be trapped by the vesicles during their preparation.

The protein composition of the low-density vesicles was further characterized by identifying the wheat germ agglutinin binding proteins. Wheat germ agglutinin is a lectin which binds to glycoproteins containing *N*-acetylglucosamine. The proteins of each subcellular fraction were first separated by SDS-polyacrylamide electrophoresis and then transferred onto a nitrocellulose sheet. The binding of peroxidase conjugated wheat germ agglutinin to the protein bands was visualized using the peroxidase stain, 4-chloro-1-naphthol. This *method* was not sensitive enough to detect any wheat germ agglutinin binding proteins in mitochondrial, cytosol, myofibril, or sarcoplasmic reticulum fractions but at least 6 major bands and 15 minor bands appeared in the low-density vesicle fraction indicating an enrichment of glycoproteins in this fraction (data not shown). In the presence of 0.1 M *N*-acetylglucosamine, no wheat germ agglutinin binding to the low-density vesicle fraction was observed.

The location of the proteins in the low density vesicles was investigated using trypsin digestion and fluorescamine labeling of intact and solubilized membranes. Addition of trypsin to intact vesicles resulted in the rapid digestion of the 200 000 and 100 000 M_w proteins (Fig. 3). The

TABLE II

LATENT ACTIVITY OF CYTOSOL ENZYMES IN THE LOW-DENSITY VESICLES

Aldolase, lactate dehydrogenase, creatine phosphokinase and pyruvate kinase activities in the low density vesicles and cytosol fraction were assayed in KCl solution with and without 0.1% Triton X-100 as described in Methods.

	Enzyme activity (μmol/mg min)			
	Aldolase	Lactate dehydrogenase	Creatine phosphokinase	Pyruvate kinase
Low-density vesicles				
– detergent	0.5	0.09	1.3	0.07
+0.1% Triton X-100	4.1	1.10	6.3	0.61
Cytosol				
– detergent	24.7	11.0	144	6.3
+0.1% Triton X-100	24.7	11.0	144	6.3

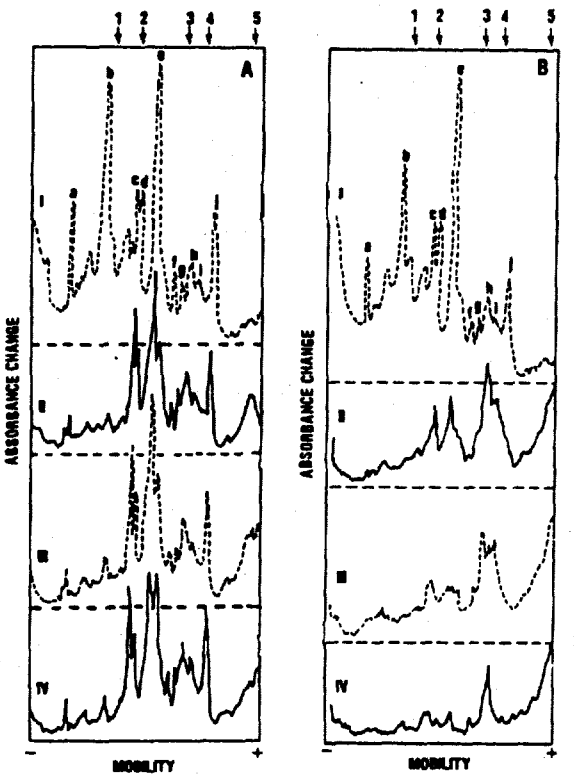

Fig. 3. Digestion of low-density vesicles with trypsin. (A) Low-density vesicles (4.5 mg/ml) were incubated in 0.15 M KCl, 10 mM Mops, 5 mM $MgSO_4$ at 25°C. Aliquots (50 μl) were removed before (I), or 1 min (II), 10 min (III), or 100 min (IV), after the addition of trypsin (2 μg/ml). PMSF (0.2 mM) was immediately added to the aliquots to inhibit the trypsin. After all the aliquots were collected, they were analyzed by SDS-polyacrylamide gel electrophoresis as described in Methods. The gels were stained with Coomassie blue, destained and scanned with a Gelford gel scanner at 550 nm. Mobilities of the molecular weight standards are indicated by the arrows: 1, phosphorylase *b*; 2, bovine serum albumin; 3, ovalbumin; 4, carbonic anhydrase; 5, soybean trypsin inhibitor. (B) Same as A, except low density vesicles were solubilized with 5 mg/ml deoxycholate before the trypsin addition.

56 000 M_w protein appeared to be cleaved to form a protein of about 51 000 M_w. Most of the other proteins seem to be unaffected by trypsin. The Mg^{2+}-ATPase activity was not influenced by trypsin even at a concentration of 1 mg/ml incubated for 30 min at 25°C. After solubilization the low-density vesicles with deoxycholate, all the proteins became susceptible to proteolytic digestion with the exception of a 35 000 M_w protein. The addition of the nonpermeable cycloheptaamylose-fluorescamine complex to intact vesicles predominantly labeled the 100 000 and 56 000 M_w proteins (Fig. 4). Under the same conditions the Mg^{2+}-ATPase was inhibited 55%. All the proteins appeared to be labeled after the membranes were solubilized with sodium dodecyl sulfate (Fig. 4). These experiments indicate that the 100 000 and 56 000 M_w proteins are exposed to the external medium while most of the other proteins become exposed only after disruption of the vesicle membrane.

Since the specific activity of purified Mg^{2+}-ATPase is not known, the percentage of the vesicles in the low density vesicle fraction which actually contains the Mg^{2+}-ATPase cannot be estimated. The high content of cholesterol, 5'-nucleotidase and glycoproteins in the low-density vesicle fraction suggests that at least some of the vesicles are

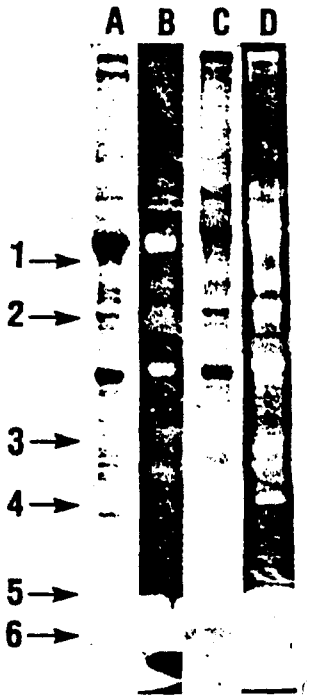

Fig. 4. Fluorescamine labeling of low-density vesicles. (Lanes A and B). Low-density vesicles (2 mg protein/ml) were incubated in 0.25 M sucrose, 10 mM imidazole (pH 7.5) and 2.5 mg/ml cycloheptaamylose-fluorescamine for 30 min at 37°C. After glycine (0.25 M) was added to react with the remaining fluorescamine, 5% SDS and 1% β-mercaptoethanol were added and the sample was heated at 100°C for 5 min. A 40-μl aliquot was then removed and analyzed by SDS-polyacrylamide electrophoresis. The gel was photographed under ultraviolet light with the shutter opened for 1 min to detect the proteins labeled with fluorescamine (lane B) and then the proteins stained with Coomassie brilliant blue R-115 (lane A). (Lanes C and D) Same as lanes A and B except 0.2% SDS was included in the fluorescamine incubation solution to solubilize the low-density vesicles. Mobilities of the molecular weight standards are indicated by the arrows: 1, phosphorylase *b* (94000); 2, bovine serum albumin (67000); 3, ovalbumin (43000); 4, carbonic anhydrase (30000); 5, soybean trypsin inhibitor (20000); and 6, α-lactalalbumin (14000).

derived from the plasma membrane and/or the transverse tubule. However, the low-density vesicle fraction may contain membranes from other sources, so the localization of the Mg^{2+}-ATPase is not possible at this time.

Electron micrographs of the low density fraction indicated a heterogeneous population of vesicles of various sizes present in the low-density fraction.

Rate of ATP hydrolysis by the Mg^{2+}-ATPase

The rate of ATP hydrolysis by the Mg^{2+}-ATPase as monitored by the enzyme coupled assay was nonlinear but declined exponentially (first-order rate constant $\cong 0.2\ min^{-1}$ at 37°C) (Fig. 5). Similar results were obtained when ATP hydrolysis was assayed by measuring the rate of P_i release from [γ-^{32}P]ATP. Addition of 2 mM K_2HPO_4 had no effect on the Mg^{2+}-ATPase activity, indicating that the decline in ATPase activity is not due to phosphate release from ATP. In the coupled enzyme assay, ATP is regenerated from ADP by pyruvate kinase and phospho*enol*pyruvate, so the decay in ATPase activity was not due to ADP accumulation. The initial rate of ATP hydrolysis was found to be directly proportional to the protein concentration of the low-density vesicles from 1 to 5 μg/ml using the coupled enzyme assay and from 10 to 100 μg/ml using the [γ-^{32}P]ATP assay. The rate of inactivation was independent of the protein concentration.

In the absence of ATP, the rate of inactivation was 600-times slower than that in the presence of ATP (Figs. 5 and 6). The rate of inactivation of the Mg^{2+}-ATPase was also accelerated by the addition of the non-hydrolyzable ATP analogue Ado*PP*[NH]*P* (Fig. 7). When added together with ATP, Ado*PP*[NH]*P* was a competitive inhibitor

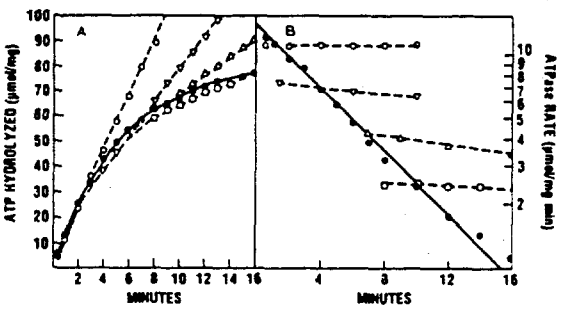

Fig. 5. Rate of ATP hydrolysis by the Mg^{2+}-ATPase. (A) Rate of ATP hydrolysis by Mg^{2+}-ATPase. ATP hydrolysis was measured by the enzyme coupled assay at 37°C in medium containing 0.15 M KCl, 10 mM ADA, 10 mM Mops (pH 6.8), 5 mM $MgSO_4$, 0.5 mM phospho*enol*pyruvate, 16 U/ml pyruvate kinase, 5 U/ml lactate dehydrogenase, 0.15 mM NADH, 2.0 mM ATP, 1.5 mM EGTA and 1 μg protein/ml low-density vesicles (●). Wheat germ agglutinin (20 μg/ml) was added before ATP (○) or 1.5 (▽), 6 (△), or 7 (□) min after ATP addition. (B) Data from panel A replotted on a logarithmic graph.

TABLE III

EFFECT OF ATP PRETREATMENT ON THE Mg^{2+}-ATPase ACTIVITY

Low-density vesicles (20 ml, 13.5 μg protein/ml) were incubated 30 min at 25°C in 0.15 M KCl, 10 mM Mops (pH 6.8), 5 mM $MgSO_4$ 1 mM EGTA, 5 mM ATP. A control sample was incubated in medium lacking the ATP. The samples were then centrifuged 130000 × *g* for 30 min and the pellet was resuspended in KCl solution at a final protein concentration of 0.6 mg/ml. Aliquots were removed from the resuspended vesicles at various times to assay *for* ATPase activity as described in Fig. 5.

Preincubation medium	Time after preincubation (min)	Initial rate of ATP hydrolysis	Inactivation rate (min^{-1})
Control	5	21.9	0.21
	30	23.2	0.21
	150	19.2	0.19
+ATP	5	5.5	0.10
	30	5.0	0.10
	150	6.8	0.11

of ATP hydrolysis by the Mg^{2+}-ATPase (K_i = 0.26 mM, data not shown), but when added in the absence of ATP, Ado*PP*[NH]*P* caused inactivation of the Mg^{2+}-ATPase.

The K_m of the Mg^{2+}-ATPase for ATP was

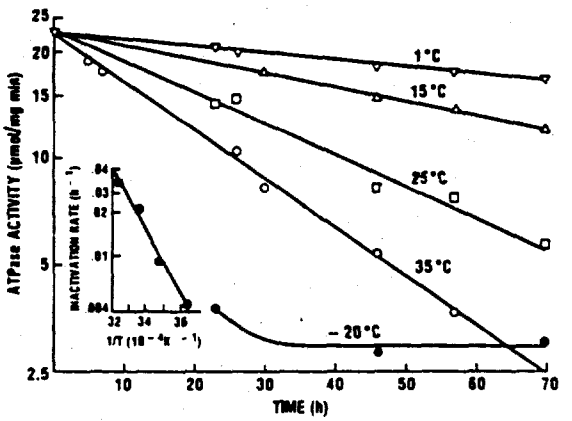

Fig. 6. Rate of inactivation of Mg^{2+}-ATPase in the absence of ATP. Low-density vesicles (26 μg protein/ml) were incubated at the indicated temperature in 0.15 M KCl, 10 mM ADA, 10 mM Mops (pH 6.8), 5 mM $MgSO_4$, 5 mM sodium azide. Aliquots (50 μl) were removed at various times and the initial ATPase activity was measured by the coupled enzyme assay at 25°C.

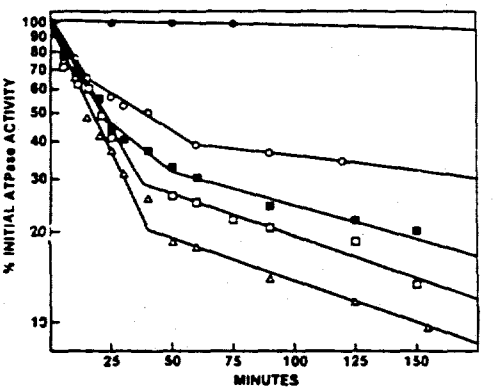

Fig. 7. Rate of inactivation of the Mg^{2+}-ATPase in the presence of Ado*PP*[NH]*P*. Low-density vesicles (0.6 mg/ml) were incubated at 25°C in 0.15 M KCl, 10 mM Mops, 10 mM ADA (pH 6.8) 5 mM $MgSO_4$ and either 0.1 mM (○), 0.2 mM (■), 0.4 mM (□) or 2.0 mM (△) Ado*PP*[NH]*P*. The control lacked Ado*PP*[NH]*P* (●). At various times aliquots (10 μl) were removed and assayed for ATPase activity using the coupled enzyme assay at 37°C. The data is reported as the ratio of the initial rate of ATP hydrolysis at the various times to the initial rate of ATP hydrolysis at $t = 0$ of the sample lacking Ado*PP*[NH]*P*. The vesicle suspension was diluted 200-fold into the assay medium so that the highest concentration of Ado*PP*[NH]*P* in the assay medium was 10 μM which did not *significantly* effect the ATPase activity (Ado*PP*[NH]*P* is a competitive inhibitor of the Mg^{2+}-ATPase with a K_i = 0.26 mM).

determined to be 0.2 mM. The rate of ATP hydrolysis and the rate of ATP-dependent inactivation did not vary between pH 5.5 and 8.5. The rate of ATP hydrolysis and the rate of ATP-dependent inactivation assayed with [γ-^{32}P]ATP was not significantly altered when the 0.15 M KCl in the assay medium was replaced with any of the following: 0.15 M NaCl, 0.15 M LiCl, 0.15 M RbCl, 0.15 M CsCl, 0.15 M sodium acetate, 0.15 M sodium bicarbonate, 0.15 M sodium aspartate, 0.15 M disodium maleate, 0.15 M sodium isothiocyanate, 0.15 M lysine chloride or 0.3 M sucrose. Various ionophores (gramicidin, valinomycin, monensin, A23187, CCCP, FCCP, dinitrophenol) and inhibitors of other ATPase enzymes (oligomycin, ouabain, vanadate, quercetin, sodium azide, sodium arsenate) had no significant effect on the effect on the activity of the Mg^{2+}-ATPase. Neither the rate of ATP hydrolysis nor the rate of ATP-dependent inactivation was significantly influenced

by 0.1 mM cytocholasin B, 0.1 mM vinblastin or 10 μM colchicine. No apparent alteration of the protein composition of the low-density vesicles as analysed by SDS-polyacrylamide electrophoresis was observed after treatment with ATP (data not shown). Neither the serine protease inhibitor phenylmethylsulfonyl fluoride nor the sulfhydryl reagents 5,5′-dithiobis(2-nitrobenzoic acid) acid and *N*-ethylmaleimide had any effect on the ATP-dependent inactivation rate of the Mg^{2+}-ATPase.

The effect of temperature on ATP hydrolysis by the Mg^{2+}-ATPase is shown in Fig. 8. The energy of activation for ATP hydrolysis and ATP-dependent inactivation determined from an Arrhenius plot of the data in Fig. 8 was 4.0 kcal/mol and 14.4 kcal/mol, respectively.

Effect of lectins on the Mg^{2+}-ATPase activity

The ability of lectins to influence the activity of the Mg^{2+}-ATPase was investigated. Of the lectins tested, only wheat germ agglutinin and concanavalin A altered the Mg^{2+}-ATPase activity. Wheat germ agglutinin and concanavalin A bind *N*-acetylglucosamine and D-mannose residues, respectively. Lectins from *Limulus polyhemus, Pisum sativum, Arachis hypogaea* and *Glycine max* had no effect on the Mg^{2+}-ATPase concentrations up to 50 μg/ml protein. Wheat germ agglutinin and concanavalin A were able to completely block ATP-dependent inactivation (Table IV). They were also able to block the inactivation of the Mg^{2+}-ATPase induced by Ado*PP*[NH]*P* (Table V). If wheat germ agglutinin was added to the assay medium following ATP addition, further inactivation was prevented, but the initial rate of ATP hydrolysis was not restored (Fig. 5). Similar results were obtained with concanavalin A. Inhibition of ATP-dependent inactivation of the Mg^{2+}-ATPase by lectins was completely reversible. Addition of 0.1 M *N*-acetylglucosamine to the assay medium eliminated the effect of wheat germ agglutinin on the Mg^{2+}-ATPase activity even when added after ATP hydrolysis is initiated. Similar results were obtained when α-methyl mannoside was added to the assay medium containing concanavalin A. These results indicate that wheat germ agglutinin and concanavalin A must bind to the membrane in order to prevent the inactivation of the Mg^{2+}-ATPase and that the effect of these lectins on the Mg^{2+}-ATPase is completely reversible.

Concanavalin A and wheat germ agglutinin shifted the K_m of the Mg^{2+}-ATPase for ATP from 0.2 mM to 0.34 mM.

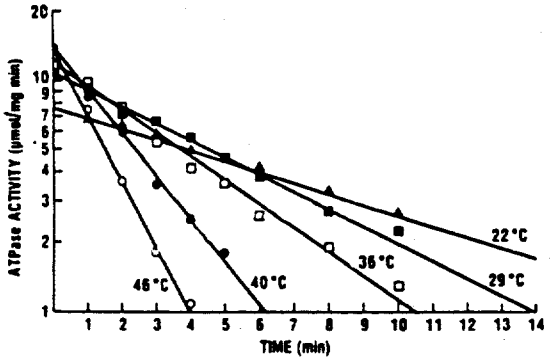

Fig. 8. Rate of inactivation of the Mg^{2+}-ATPase in the presence of ATP. ATPase activity was measured by the coupled enzyme assay at the indicated temperature in medium containing 0.15 M KCl, 10 mM ADA, 10 mM Mops (pH 6.8), 5 mM $MgSO_4$, 0.5 mM phospho*enol*pyruvate, 16.8 U/ml pyruvate kinase, 4.8 U/ml lactate dehydrogenase, 0.15 mM NADH, 2.0 mM ATP, 1.5 mM EGTA and 1.7 μg protein/ml low-density vesicles. The rate of ATP hydrolysis was determined from the change in the NADH absorbance at 340 nm.

TABLE IV

EFFECT OF WHEAT GERM AGGLUTINIIN, CONCANAVALIN A AND RABBIT ANTISERUM ON THE Mg^{2+}-ATPase ACTIVITY

Mg^{2+}-ATPase was assayed as described in Fig. 5. Low-density vesicles (1.8 μg/ml) were added to the assay medium 1 min before the addition of 2 mM ATP. When tested, the lectins, sugars, antiserum or control serum were added to the assay medium before the addition of the low-density vesicles.

Addition	Initial rate ATP hydrolysis (μmol/mg per min)	Inactivation rate (min^{-1})
1 Control	8.9	0.26
2 + wheat germ agglutinin (70 μg/ml)	5.9	0
3 + wheat germ agglutinin (70 μg/ml) and *N*-acetylglucosamine (0.1 M)	7.3	0.29
4 + concanavalin A (40 μg/ml)	6.9	0
5 + concanavalin A (40 μg/ml) and α-methylmannoside (0.1 M)	7.6	0.35
6 + rabbit antiserum (1 : 700)	5.8	0
7 + control serum (1 : 700)	10.1	0.23

TABLE V

EFFECT OF WHEAT GERM AGGLUTININ, CONCANAVALIN A AND RABBIT ANTISERUM ON Ado*PP*[NH]*P*-INDUCED INACTIVATION OF THE Mg^{2+}-ATPase

Low-density vesicles (0.38 mg protein/ml) were incubated at 25°C in KCl solution with the indicated additions for 60 min. The vesicles were then diluted 400-fold into Mg^{2+}-ATPase assay medium and the initial rate of ATP hydrolysis was determined as described in Fig. 5.

Incubation medium	ATPase activity (% of control)
Control (no Ado*PP*[NH]*P*)	100
+ 2 mM Ado*PP*[NH]*P*	26
+ 2 mM Ado*PP*[NH]*P* and wheat germ agglutinin (1 mg/ml)	91
+ 2 mM Ado*PP*[NH]*P* and wheat germ agglutinin (1 mg/ml) and *N*-acetylglucosamine (33 mM)	49
+ 2 mM Ado*PP*[NH]*P* and concanavalin A (2.5 mg/ml)	84
+ 2 mM Ado*PP*[NH]*P* and concanavalin A (2.5 mg/ml) and α-methyl mannoside (33 mM)	26
+ 2 mM Ado*PP*[NH]*P* and rabbit antiserum (1 : 100)	85
+ 2 mM Ado*PP*[NH]*P* and control serum (1 : 100)	30

Effect of rabbit antiserum to the low-density vesicles on the Mg^{2+}-ATPase activity

The effect of rabbit antiserum produced against the low density vesicles on the Mg^{2+}-ATPase activity was similar to that of wheat germ agglutinin and concanavalin A. The initial rate of ATP hydrolysis was slightly decreased by the antiserum, but the ATP-dependent inactivation was completely blocked (Table VI). Control serum had little effect on the Mg^{2+}-ATPase activity. Rabbit antiserum also prevented inactivation of the Mg^{2+}-ATPase by Ado*PP*[NH]*P* (Table VI). Like the wheat germ agglutinin, rabbit antiserum was found to bind to a variety of proteins in the low density fraction (data not shown).

Effect of glutaraldehyde on the Mg^{2+}-ATPase activity

Glutaraldehyde is a cross-linking reagent which is able to react with amine groups of protein and lipids. Immediately after adding 2.5% glutaraldehyde to a suspension of low-density vesicles at 1°C, the initial rate of ATP hydrolysis and the rate of ATP-dependent inactivation decreased 36% and 54%, respectively (Fig. 9). After a 30 min incuba-

TABLE VI

EFFECT OF WHEAT GERM AGGLUTININ, CONCANAVALIN A, AND RABBIT ANTISERUM ON THE INCUBATION OF THE Mg^{2+}-ATPase IN THE PRESENCE OF DETERGENTS

Mg^{2+}-ATPase activity was measured as described in Fig. 10 except wheat germ agglutinin (20 μg/ml), concanavalin A (50 μg/ml) and rabbit antiserum (1 : 700) were included in the assay medium where indicated. Not determined, N.D.

Detergent	Control		Wheat germ agglutinin		+ Concanavalin A		+ Rabbit antiserum	
	Initial ATPase rate (min^{-1}) (%)	Inactivation rate	Initial ATPase rate (%)	Inactivation rate (min^{-1})	Initial ATPase rate (%)	Inactivation rate (min^{-1})	Initial ATPase rate (%)	Inactivation rate (min^{-1})
-	100	0.28	75	0	95	0	102	0
25 μg/ml Brij 35	96	0.75	83	0	95	0	87	0
100 μg/ml Brij 35	85	1.76	83	0	94	0	75	0
2000 μg/ml Brij 35	120	1.54	83	0.08	94	0.07	N.D.	N.D.
100 μg/ml Chapso	93	0.41	65	0	88	0	91	0
250 μg/ml Chapso	82	1.62	65	0.05	79	0	70	0.05
1000 μg/ml Chapso	-	< 3	56	0.14	41	0.1	58	0.12
1 μg/ml Triton X-100	94	0.29	75	0	90	0	88	0
10 μg/ml Trison X-100	85	0.42	63	0	92	0	96	0
50 μg/ml Triton X-100	60	0.76	47	0.06	77	0.09	94	0.10

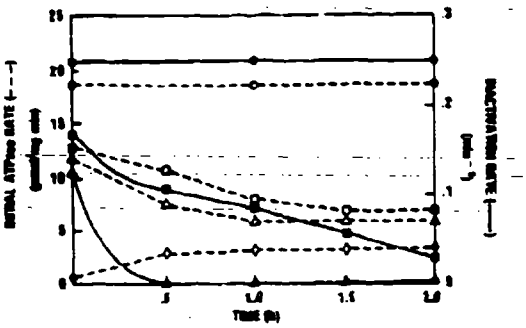

Fig. 9. Effect of glutaraldehyde on Mg^{2+}-ATPase activity. Low-density vesicles (0.2 mg protein/ml) were incubated at 1°C in 0.15 M KCl, 10 mM Mops (pH 6.8), 5 mM $MgSO_4$ and 2.5% (▲, △, ◇) or 0.25% (■, □) glutaraldehyde. Controls lacked glutaraldehyde (●, ○). Aliquots (5 μl) were removed at various times and diluted into 2 ml of ATPase assay medium to determine the initial rate of ATP hydrolysis (○, △, □, ◇) and the rate of inactivation (●, ▲, ■) as described in Fig. 5. In one experiment (◇), the vesicles incubated in 2.5% glutaraldehyde were assayed in medium containing 0.1% Triton X-100 in order to measure detergent-resistant ATPase.

tion in 2.5% glutaraldehyde, the Mg^{2+}-ATP showed no ATP-dependent inactivation but the initial rate of ATP-hydrolysis was reduced by 58%. Similar results were obtained in 0.25% glutaraldehyde, except the rate at which ATP-dependent inactivation was inhibited was greatly reduced (Fig. 9).

The Mg^{2+}-ATPase of low-density vesicles not treated with glutaraldehyde was completely inhibited by 0.1% Triton X-100. But after an hour incubation with 2.5% glutaraldehyde at 1°C, 1% Triton X-100 inhibited the Mg^{2+}-ATPase by only 42% (Fig. 9). In conclusion, cross-linking the membrane components with glutaraldehyde of the low-density vesicles (1) completely blocked ATP-dependent inactivation while inhibiting the initial rate of ATP hydrolysis up to 68%, and (2) increased the resistance of the Mg^{2+}-ATPase to detergents.

Several other cross-linking reagents which were tested (dimethyl pimelimidate, dimethyl 3,3'-dithiobis(propionimidate), 2-iminothiolane, disuccinimidyl suberate, and ethylene glycol bissuccinimicyl succinate) also prevented inactivation. When incubated with the low density vesicles at a concentration of 50–5 mM in 0.1 M triethylamine (pH 8.0) for 30 min at 25°C, they reduced the initial rate of ATP hydrolysis of the Mg^{2+}-ATPase 5–90% and completely eliminated ATP-dependent inactivation. Glutaraldehyde (50 mM) under the same conditions reduced the initial rate by 44%.

Effect of detergents on the Mg^{2+}-ATPase activity

At low concentrations, detergents maybe incorporated into biological membranes affecting membrane fluidity and protein-lipid interaction. At higher concentrations, some detergents can totally disrupt the membrane leading to the formation of micelles containing varying amounts of lipid, protein and detergent. At low concentrations of detergents and short incubation times, the initial rate of Mg^{2+}-ATPase was only slightly altered, while the rate of ATP-dependent inactivation was greatly accelerated. Fig. 10 shows the effect of Chapso, Brij 35 and Triton X-100 on the Mg^{2+}-ATPase activity. Similar results were obtained with Tween 20, Tween 40, Tween 60, Tween 80, Nonidet P-40, cholate, Chaps, Digitonin, Brij 76, Brij 99, Zwittergent 3-08, Zwittergent 3-10, Zwittergent 3-12, Zwittergent 3-14, Zwittergent 3-16, octylglucoside

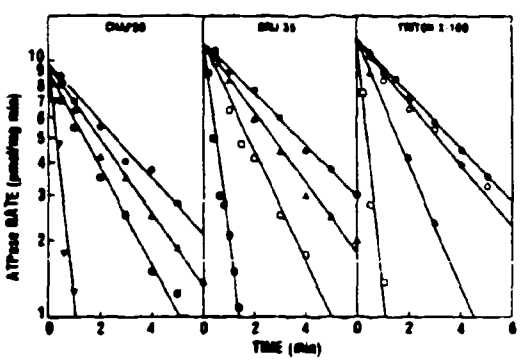

Fig. 10. Effect of Chapso, Brij 35 and Triton X-100 on Mg^{2+}-ATPase activity was measured by the coupled enzyme assay at 37°C in medium containing 0.15 M KCl, 10 mM ADA, 10 mM Mops (pH 6.8), 5 mM $MgSO_4$, 16 U/ml pyruvate kinase, 5 U/ml lactate dehydrogenase, 0.5 mM phospho*enol*pyruvate and 0.15 M NADH. Chapso, Brij 35 or Triton X-100 was added to the assay medium at a final concentration of 0.00025% (○), 0.001% (△), 0.0025% (□), 0.01% (■) or 0.025% (▼). The control (●) lacked detergent. Low-density vesicles (3.4 μg protein/ml) were added 1 min before the reaction was initiated with 2 mM ATP. The rate of ATP hydrolysis was determined from the rate of NADH oxidation as monitored spectrophotometrically at 340 nm.

and lysophosphatidylcholine. Some detergents such as Brij 35 and Tween 80 were unable to solubilize the Mg^{2+}-ATPase even at high concentrations (the Mg^{2+}-ATPase was still precipitable by centrifugation at 100000 × *g* for 10 min). These detergents increased the inactivation rate 10-fold at a concentration of 0.05% (3.4 μg protein/ml low-density vesicles) but additional increases in the detergent concentration had no effect. Wheat germ agglutinin, concanavalin A or antiserum prevented the ATP-dependent inactivation of the Mg^{2+}-ATPase even in the presence of 2% Brij 35 (Table VI). Other detergents such as Chapso, Triton X-100, Nonidet P-40, cholate, octylglucoside and Zwittergent 3-16 completely solubilized the membrane at high detergent to protein ratios, at which no Mg^{2+}-ATPase activity was observed. At low detergent concentrations, the inactivation rate was increased with little change in the initial rate of ATP hydrolysis. Wheat germ agglutinin, concanavalin A or antiserum could still block the ATP-dependent inactivation of the Mg^{2+}-ATPase at low concentrations of Chapso and Triton X-100, but inactivation still occurred at higher concentrations (Table VI).

Discussion

The Mg^{2+}-ATPase of rat skeletal muscle had the unusual property of ATP-dependent inactivation. Inactivation could also be induced by the nonhydrolyzable ATP analogue Ado*PP*[NH]*P*. The rate of ATP-dependent inactivation was increased by detergents (Fig. 10) and temperature (Fig. 8). Inactivation was inhibited by wheat germ agglutinin (Fig. 5), concanavalin A (Table IV), glutaraldehyde (Fig. 9) and rabbit antiserum produced against the low-density vesicles (Table IV). Since ATP-dependent inactivation is blocked by cross-linking components of the low-density vesicle membrane with lectins, antibodies or glutaraldehyde, mobility of the membrane proteins may be required for inactivation (Fig. 11). The active Mg^{2+}-ATPase may be a protein complex which dissociates to give inactive monomers. Dissociation would be prevented by cross-linking the complex with wheat germ agglutinin, concanavalin A, antibodies or glutaraldehyde. ATP or Ado*PP*[NH]*P* would promote dissociation. Detergents would increase the rate of dissociation. Alternatively, the Mg^{2+}-ATPase may be regulated by a separate protein which must interact with the Mgl^{2+}-ATPase to inactivate it. Preventing protein mobility with cross-linking reagents, lectins or antiserum would block the interaction of the regulatory protein with the Mg^{2+}-ATPase. Inactivation of the Mg^{2+}-ATPase by the regulatory protein would require ATP or Ado*PP*[NH]*P*. A third possibility is that the Mg^{2+}-ATPase exists in two conformational states, active and inactive. The inactive state would be stabilized by ATP or Ado*PP*[NH]*P*, while the active state would be stabilied by the binding of lectins or antibodies to the Mg^{2+}-ATPase. At the present time, it is not possible to eliminate any of these proposed mechanisms for the regulation of the Mg^{2+}-ATPase without further experimental data.

Since there is an abundance of ATP in the muscle cell, something must prevent the inactivation of the Mg^{2+}-ATPase in vivo. One possibility is that the Mg^{2+}-ATPase is not normally exposed to ATP. There are numerous reports in the literature on the existence of ecto-ATPase enzymes which act on extracellular substrates [19–24]. If the vesicles which contain the Mg^{2+}-ATPase are nonpermeable to ATP and lectins, then the ATP and lectin binding sites must be on the same side of the membrane. Since the extracellular surface of muscle cells is heavily glycosylated, this would be the most likely site of lectin binding. Therefore it is possible that the active site of the Mg^{2+}-ATPase faces the extracellular medium rather than hydrolyzing intracellular ATP. A large fraction of the low density vesicles appear to be nonpermeable since (1) most of the proteins associated with the intact vesicles were protected from trypsin digestion (Fig. 3) and from labeling with cyclohepatamylose-fluorescamine (Fig. 4), (2) a 6–10-fold increase in the activity of cytoplasmic enzymes trapped inside the low-density vesicles was observed after disrupting the membrane with detergent (Table II), and (3) the efflux rate of ^{86}Rb (0.5 min^{-1}) from the vesicles was relatively slow (data not shown). It is not known, however, if the Mg^{2+}-ATPase is associated with these tight vesicles.

Another possible way in which the Mg^{2+}-ATPase retains its activity in vivo is that inactiva-

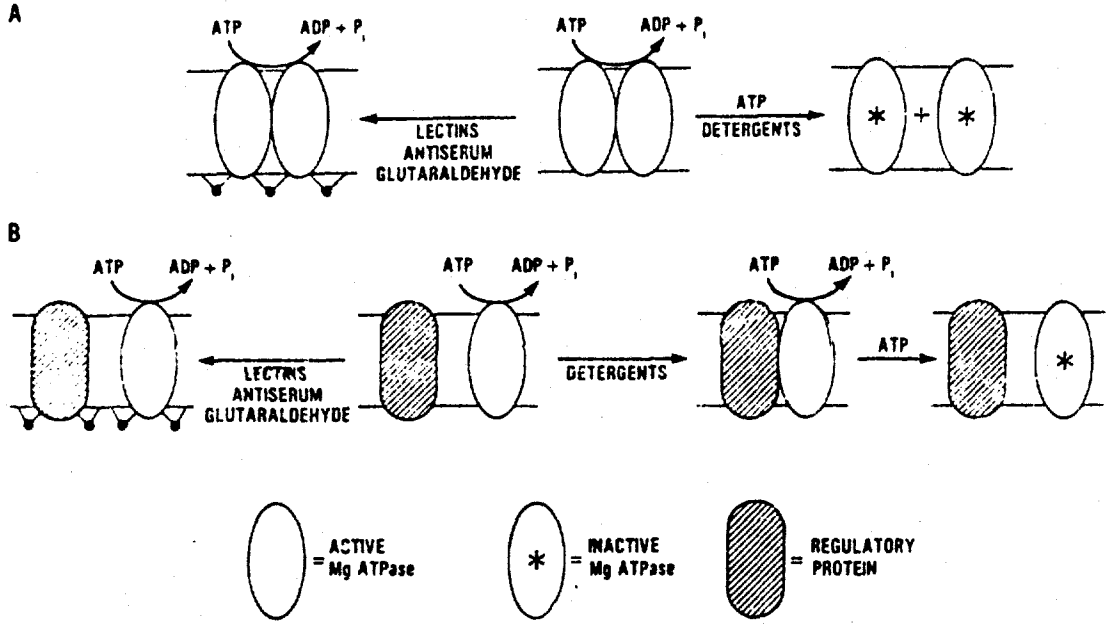

Fig. 11. Regulation of Mg^{2+}-ATPase. Mechanism A. Active Mg^{2+}-ATPase is a protein complex. Dissociation of the protein complex is promoted by ATP and detergents and leads to inactivation of the ATPase. Lectins, antiserum and glutaraldehyde prevent dissociation of the protein complex. Mechanism B. Mg^{2+}-ATPase is inactivated by a regulatory protein in the presence of ATP. Lectins, antiserum and glutaraldehyde immobilize membrane proteins preventing the interaction between the Mg^{2+}-ATPase and the regulatory protein. Low concentrations of detergents increase the mobility of proteins in the membrane and therefore increase the rate of inactivation.

tion may be blocked by a naturally occurring regulatory protein in a similar manner in which lectins, antiserum or glutaraldehyde prevent inactivation. No such regulatory protein, however, was detected in the muscle cytosol fraction or rat serum.

During the preparation of the low density vesicles, inactivation is partially prevented by working at 4°C, but it is likely that some inactivation does occur. When the Mg^{2+} concentration of the isolation medium was maintained below 1 μM with EDTA to inhibit the Mg^{2+}-ATPase, the specific activity of the Mg^{2+}-ATPase in the low density vesicles was increased 3-fold. EDTA was not routinely added to the isolation medium since it also caused an increase in the contamination of the low-density vesicle fraction with sarcoplasmic reticulum.

The Mg^{2+}-ATPase found in the low-density vesicles was not specific for skeletal muscle (unpublished data). A Mg^{2+}-ATPase with very similar properties as the skeletal muscle enzyme was also found in low density vesicles isolated from heart, spleen, lung, kidney, liver, brain and adipose tissue. The Mg^{2+}-ATPase activity of low density vesicles from heart, spleen and adipose tissue had a specific activity equal to or greater than that from skeletal muscle.

The function of the Mg^{2+}-ATPase is not known. We have found no evidence that the Mg^{2+}-ATPase is involved in ion transport. The enzyme requires millimolar amounts of Mg^{2+} or Ca^{2+} for activity but no other ionic requirements were observed. The activity of the ATPase was not influenced by a variety of anions, monovalent cations or ionophores. The efflux rate of ^{86}Rb from the low-density vesicles was not influenced by ATP nor was ATP-dependent Ca^{2+} uptake into the vesicles observed. The rate of ATP hydrolysis by the low-density vesicles was not influenced by preimposed negative or positive membrane potentials generated with Cl^- or K^+ gradients.

We are presently involved in developing techniques to solubilize and purify active Mg^{2+}-ATPase from skeletal muscle in order to better characterize this enzyme.

Acknowledgements

This work was supported by research grants from the National Institutes of Health (GM 29300), from the Office of Naval Research and by the Uniformed Services University of the Health Sciences. The collaboration of Miss Shirley Lee is gratefully acknowledged.

References

1 Fernandez, J.L., Rosemblatt, M. and Hidalgo, C. (1980) Biochim. Biophys. Acta 599, 552–568
2 Scales, D. and Sabbadini, R. (1979) J. Cell Biol. 83, 33–46
3 Flaherty, J.O., Barrett, E.J., Bradley, D.P. and Headon, D.R. (1975) Biochim. Biophys. Acta 401, 177–183
4 Rosemblatt, M., Hidalgo, C., Vergara, C. and Ikemoto, N. (1981) J. Biol. Chem. 256, 8140–8148
5 Malouf, N.N. and Meissner, G. (1979) Exp. Cell Res. 122, 233–250
6 Gilbert, J.R. and Meissner, G. (1982) J. Membrane Biol. 69, 77–84
7 Warren, G.B., Toon, P.A., Birdsall, N.J., Lee, A.G. and Metcalfe, J.C. (1974) Proc. Natl. Acad. Sci. U.S.A. 71, 622–626
8 DeMeis, L. and Carvalho, M.C. (1974) Biochemistry 13, 5032–5038
9 Courchaine, A.J., Miller, W.H. and Stein, D.B. (1959) Clin. Chem. 5, 609–614
10 Bligh, E.G. and Dyer, W.J. (1959) Can J. Biochem. Physiol. 37, 911–917
11 Bartlett, G.R. (1959) J. Biol. Chem. 234, 466–468
12 Sibley, J.A. and Lehninger, A.L. (1949) J. Biol. Chem. 177, 859–872
13 Bücher, T. and Pfleiderer, G. (1955) in Methods in Enzymology (Colowick, S.P. and Kaplan, N.O., eds.), Vol. 1, pp. 435–440, Academic Press, New York
14 Stolzenbach, F. (1966) in Methods in Enzymology (Wood, W.A., ed.), Vol. 9, pp. 278–288, Academic Press, New York
15 Rosalki, S.B. (1967) J. Lab. Clin. Med. 69, 696–705
16 Dixon, T.F. and Purdom, M. (1954) J. Clin. Pathol. 7, 341–343
17 Laemmli, U.K. (1970) Nature 227, 680–685
18 Hawkes, R. Niclay, E. and Gordon, J. (1982) Anal. Biochem., 119, 142–147
19 Wallach, D.F. and Ullrey, D. (1962) Biochim. Biophys. Acta 64, 526–539
20 DePierre, J. and Karnovsky, M.L. (1973) J. Cell Biology 56, 275–303
21 Trans, E.G. and Lauter, C.J. (1974) Biochim. Biophys. Acta 345, 180–197
22 DePierre, J. and Karnovsky, M.L. (1974) J. Biol. Chem. 249, 7111–7120
23 Ronquist, G. and Agren, G.K. (1975) Cancer Res. 35, 1402–1406
24 Karaski, S. and Okigaki, J. (1976) Cancer Res. 36, 4491–4499
25 O'Farrell, P.H. (1975) J. Biol. Chem. 250, 4007–4021

J. Membrane Biol. 78, 73–79 (1984)

The Journal of
Membrane Biology

Effect of Na_3VO_4 and Membrane Potential on the Structure of Sarcoplasmic Reticulum Membrane

Troy J. Beeler*, Laszlo Dux**, and Anthony N. Martonosi**

* Department of Biochemistry, Uniformed Services University of Health Sciences, Bethesda, Maryland 20014, and
** Department of Biochemistry, State University of New York, Upstate Medical Center, Syracuse, New York 13210

Summary. Two-dimensional crystalline arrays of Ca^{2+}-ATPase molecules develop after treatment of sarcoplasmic reticulum vesicles with Na_3VO_4 in a Ca^{2+}-free medium. The influence of membrane potential upon the rate of crystallization was studied by ion substitution using oxonol VI and 3,3'-diethyl-2,2'-thiadicarbocyanine ($Di-S-C_2(5)$) to monitor inside positive or inside negative membrane potentials, respectively. Positive transmembrane potential accelerates the rate of crystallization of Ca^{2+}-ATPase, while negative potential disrupts preformed Ca^{2+}-ATPase crystals, suggesting an influence of transmembrane potential upon the conformation of Ca^{2+}-ATPase.

Key Words Ca^{2+}, Mg^{2+}-ATPase · Ca^{2+} transport · membrane potential · vanadate · crystals · sarcoplasmic reticulum

Introduction

Two-dimensional crystalline arrays of the Ca^{2+} transport ATPase develop after treatment of sarcoplasmic reticulum vesicles with Na_3VO_4 in a Ca^{2+}-free medium (Dux & Martonosi, 1983*a*). In order to form crystals the Ca^{2+}-ATPase molecules must assume the E_2 conformation, which is stabilized by vanadate. Ca^{2+} in concentration sufficient to saturate the high affinity Ca^{2+} binding site of the Ca^{2+}-ATPase prevents the formation of ATPase crystals and disrupts the crystals that were formed previously (Dux & Martonosi, 1983*a*). These effects of Ca^{2+} can be attributed to the changes in the conformation of Ca^{2+}-ATPase associated with the binding of Ca^{2+}. Based on these observations the crystallization of Ca^{2+}-ATPase may serve as an indicator of the conformational requirements of ATPase-ATPase interactions in sarcoplasmic reticulum membranes.

Artificially imposed inside positive membrane diffusion potential strongly accelerated the rate of formation of Ca^{2+}-ATPase crystals (Dux & Martonosi, 1983*b*). Inside negative potential interfered with the crystallization, and disrupted preformed Ca^{2+}-ATPase crystals. It is assumed that the membrane potential alters the conformational equilibrium of Ca^{2+}-ATPase in a manner that either promotes or hinders the interaction between ATPase molecules, depending upon the direction of the potential (Dux & Martonosi, 1983*b*). These observations may have physiological significance in light of the membrane potential changes in sarcoplasmic reticulum that accompany the uptake and release of Ca^{2+} *in vivo* (Bezanilla & Horowicz, 1975; Vergara & Bezanilla, 1981) and *in vitro* (Beeler, 1980; Beeler, Farmen & Martonosi, 1981).

Incorporation of the Ca^{2+} transport ATPase into phospholipid vesicles increases the permeability of the membrane by several orders of magnitude (Jilka, Martonosi & Tillack, 1975; Martonosi, 1975; Jilka & Martonosi, 1977). Therefore, in addition to its role in mediating ATP-dependent active Ca^{2+} transport, the Ca^{2+}-ATPase also contributes to the passive permeability of the membrane to ions and other small molecules. Considering the effect of membrane potential on ATPase-ATPase interactions (Dux & Martonosi, 1983*b*) and the potential changes associated with the uptake and release of Ca^{2+} by sarcoplasmic reticulum (Beeler et al., 1981; Vergara & Bezanilla, 1981) it is tempting to speculate that changes in the conformational equilibrium of Ca^{2+}-ATPase under the influence of membrane potential may contribute to the changes in the Ca^{2+} permeability of sarcoplasmic reticulum membrane by altering the monomer-polymer equilibrium of Ca^{2+}-ATPase (Martonosi et al., 1977; Vanderkooi et al., 1977).

As a first step to test this hypothesis we analyzed the effect of Na_3VO_4 upon the magnitude and duration of membrane potential generated by ion substitutions in rabbit sarcoplasmic reticulum vesicles, using the voltage sensitive dyes diethylthiadicarbocyanine and oxonol VI, and compared the changes in membrane potential with the rate of crystallization of Ca^{2+}-ATPase.

Materials and Methods

Sarcoplasmic reticulum vesicles were prepared from predominantly white rabbit skeletal muscle, as described earlier (Nakamura et al., 1976), with slight modifications (Beeler et al., 1981).

Diffusion potential across the sarcoplasmic reticulum membrane was generated by ion substitution, as described in detail in the text and in the Figure legends. The difference absorbances of oxonol VI (Molecular Probes, Inc., Junction City, Oregon) and 3,3'diethyl-2,2'-thiadicarbocyanine (Di−S−C_2(5)) (Eastman Kodak, Rochester, New York) were recorded on an Aminco DW-2 spectrophotometer. The absorbance changes of oxonol VI and Di−S−C_2(5) served to evaluate the changes in inside-positive and inside-negative membrane potential, respectively (Beeler et al., 1981). Oxonol VI contains delocalized negative charges and accumulates into compartments under the influence of inside positive potential, resulting in absorbance and fluorescence changes. Di−S−C_2(5), a dye with delocalized positive charges, responds in an analogous manner to inside negative potential.

For electron microscopy, the vesicle suspensions (≃1 mg protein ml) were placed on carbon-coated parlodion films and negatively stained with freshly prepared 1% uranyl acetate (pH 4.3). The specimens were viewed with a Siemens Elmiskop 102 electron microscope at 60 kV accelerating voltage. For magnification calibration catalase crystals negatively stained with 1% uranyl acetate were used.

Results

Ca^{2+}-ATPase Membrane Crystals in Sarcoplasmic Reticulum

Crystalline arrays of Ca^{2+}-ATPase develop upon exposure of sarcoplasmic reticulum vesicles to 5 mM Na_3VO_4 in a Ca^{2+}-free medium, at 2 °C (Fig. 1). The Ca^{2+}-ATPase crystals are usually observed on the surface of elongated tubules which are approximately 600 to 800 Å in diameter. The crystal lattice consists of chains of ATPase dimers which are in register with neighboring chains, and surround the tubules in a right-handed helix (Taylor, Dux & Martonosi, 1983a; Peracchia et al.[1]). The diagonal lattice arises from superimposition of the front and rear images of the collapsed cylinders. The lattice constants are: $a = 56.34$ Å, $b = 104.78$ Å and $\gamma = 72.72°$ (Taylor et al., 1983). Under the conditions described in Fig. 1, crystallization of about 2/3 of the vesicles requires 1 to 2 days.

Very much faster crystallization of the Ca^{2+}-ATPase was observed after dilution of the vesicles preincubated in 0.15 M choline chloride medium into a medium containing 0.15 M K-glutamate and 5 mM Na_3VO_4 (Fig. 2). Under these conditions outward movement of Cl^- and inward movement of K^+ generate an inside positive diffusion potential across the vesicle membrane. Within 15 sec after dilution, Ca^{2+}-ATPase crystals were observed on the surface of about half of the vesicles. Control preparations which were pre-equilibrated in K-glutamate medium, showed essentially no crystallization 15 sec after transfer into K-glutamate medium containing 5 mM Na_3VO_4 (Fig. 3). Under these conditions no potential is expected to develop, and significant crystallization requires several hours of incubation with vanadate.

These observations, together with earlier findings (Dux & Martonosi, 1983*b*), establish that conditions which are expected to generate positive membrane potential facilitate the association of ATPase molecules into extended crystalline arrays.

Fig. 1. Crystalline arrays of Ca-ATPase molecules in rabbit sarcoplasmic reticulum vesicles. Sarcoplasmic reticulum vesicles were incubated in 0.1 M KCl, 10 mM imidazole pH 7.4, 5 mM $MgCl_2$, 0.5 mM EGTA, 5 mM Na_3VO_4 at 2 °C and samples were taken for negative staining after 4 days. Magnification: 239,519 ×

[1] C. Peracchia, L. Dux & A. Martonosi. Crystallization of intramembrane particles in rabbit sarcoplasmic reticulum vesicles by vanadate. (*unpublished*)

Fig. 2. Rapid crystallization of Ca-ATPase molecules under the influence of inside positive potential. Sarcoplasmic reticulum vesicles (10 mg/ml) were preincubated in 0.15 M choline chloride, 10 mM imidazole pH 7.4, 5 mM $MgCl_2$ and 0.5 mM EGTA for 16 hr at 2 °C, and then diluted 10-fold in 0.15 M K-glutamate, 10 mM imidazole pH 7.4, 5 mM $MgCl_2$, 0.5 mM EGTA, 5 mM Na_3VO_4 containing medium. Negative staining was carried out 15 sec after dilution. Magnification: 102,651 ×

Fig. 3. Surface structure of vesicles after dilution into medium of identical composition. Sarcoplasmic reticulum vesicles (10 mg ml) were pre-incubated in 0.15 M K-glutamate, 10 mM imidazole pH 7.4, 5 mM $MgCl_2$, and 0.5 mM EGTA medium for 16 hr, then diluted 10-fold in the same medium containing 5 mM Na_3VO_4. Negative staining was completed 15 sec after dilution. Magnification: 102,651 ×

Oxonol VI Signals in Vanadate-Treated Sarcoplasmic Reticulum Vesicles after Transfer from Choline Chloride into K-Glutamate Medium

The time course of the potential change generated by transfer of vesicles from choline chloride into K-glutamate medium was followed by measuring the difference absorbance of the voltage sensitive dye oxonol VI at 625 to 586 nm (Fig. 4).

Dilution of control vesicles from K-glutamate into K-glutamate media containing 50 μM Ca (Fig. 4*A*, sample 1′) increases the absorbance by about 0.14 to 0.15 units; the absorbance change of control samples containing 5 mM vanadate (sample 2′) is significantly smaller. The absorbance change in control samples rapidly achieves a steady

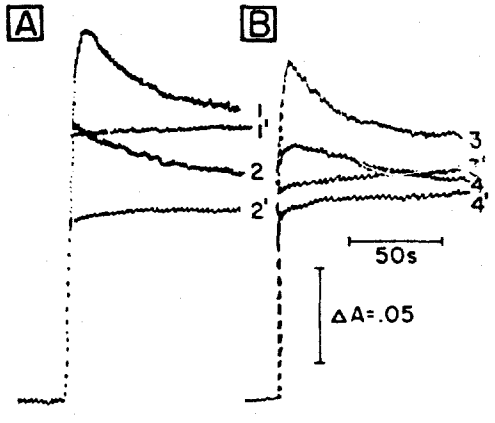

Fig. 4. Absorbance changes of oxonol VI upon dilution of vesicles pre-equilibrated in choline chloride into K-glutamate medium. Sarcoplasmic reticulum vesicles (30 mg protein ml) were equilibrated overnight at 2 °C in medium containing 0.15 M choline chloride, 10 mM histidine (pH 6.8), 5 mM $MgSO_4$, and 50 μM $CaCl_2$. Inside positive membrane potentials were generated by diluting 4 μl aliquots of this suspension into 2 ml of medium containing 0.15 M K-glutamate, 10 mM histidine (pH 6.8), 5 mM $MgSO_4$, 10 μg ml oxonol VI and: 50 μM $CaCl_2$ (trace 1); 50 μM $CaCl_2$, 5 mM Na_3VO_4 (trace 2); 1 mM EGTA (trace 3); or 1 mM EGTA, 5 mM Na_3VO_4 (trace 4). The difference absorbance of oxonol VI at 625 to 586 nm was measured in an Aminco DW-2 spectrophotometer at 10 °C. For controls, the sarcoplasmic reticulum vesicles were equilibrated in K-glutamate instead of choline chloride medium and diluted as described above (traces 1′–4′)

Fig. 5. Disruption of Ca^{2+}-ATPase membrane crystals under the influence of inside negative potential. Sarcoplasmic reticulum vesicles (10 mg/ml) were precrystallized in 0.15 M K-glutamate, 10 mM imidazole pH 7.4, 5 mM $MgCl_2$, 0.5 mM EGTA, 5 mM Na_3VO_4 medium at 2 °C for 16 hr. Under this condition 65 to 70% of the vesicles show crystalline arrays (Dux & Martonosi, 1983*b*). Negative potential was generated by 10-fold dilution of the samples in a 0.15 M choline chloride containing medium of otherwise identical composition. Magnification: 102,651 ×

level that presumably reflects the binding of oxonol VI to the sarcoplasmic reticulum vesicles in the absence of potential.

Dilution of vesicles from choline chloride into K-glutamate medium containing 50 μM Ca^{2+} (Fig. 4*A*, sample 1), causes a much greater absorbance change ($\Delta A \sim 0.20$) due to the generation of inside positive potential; this is followed by a rapid decline of the optical response as the potential is dissipated. Dilution into K-glutamate medium containing 50 μM Ca and 5 mM Na_3VO_4 (Fig. 4*A*, sample 2) gave an initial absorbance change of 0.151 which declined to a level intermediate between that of samples 1′ and 2′. The smaller absorbance change observed in the presence of vanadate (sample 2) may be due to at least two causes:

1. An effect of Na_3VO_4 on the absorbance of oxonol VI, as also reflected by the difference between the absorbance response of the two control samples (samples 1′ and 2′).

2. Na_3VO_4 decreases the potential generated by ion substitution presumably because it changes the permeability of the membrane to ions.

The difference between samples 1 and 2 cannot be attributed to crystallization of the Ca^{2+}-ATPase since 50 μM Ca^{2+} completely inhibits the formation of Ca^{2+}-ATPase crystals.

In Fig. 4*B* a similar experiment is described except that the dilution medium contained 1 mM EGTA to lower free $[Ca^{2+}]$ below 10^{-8} M. The absorbance change observed upon transfer of vesicles from choline chloride into K-glutamate medium containing EGTA is much greater in the absence (Fig. 4*B*, sample 3) than in the presence of 5 mM Na_3VO_4 (Fig. 4*B*, sample 4); in both samples the difference absorption rapidly decreases and in the presence of Na_3VO_4 (sample 4) within 1 to 2 min approaches the level of the corresponding control (sample 4′) without preimposed potential. In the absence of vanadate (sample 3) the potential signal reaches a relatively steady level 2 min after dilution, that is significantly greater than in the control (sample 3′) without pre-imposed potential. These observations imply that the signal of oxonol VI to inside positive potential generated by ion substitution is small and short-lived in the presence of EGTA and Na_3VO_4, and within 2 min the potential is largely dissipated. Therefore conditions that promote the crystallization of Ca^{2+}-ATPase decrease the potential response of oxonol VI to ion substitution, presumably by changing the ion permeability of sarcoplasmic reticulum.

Influence of Inside Negative Potential upon Preformed Ca^{2+}-ATPase Crystals

Ca^{2+}-ATPase crystals were formed by incubation of sarcoplasmic reticulum vesicles in a medium of 0.15 M K-glutamate, 10 mM imidazole pH 7.4, 5 mM $MgCl_2$, 0.5 mM EGTA and 5 mM Na_3VO_4 at 2 °C for 16 hr. About 2/3 of the vesicles showed crystalline arrays similar to those in Fig. 1 on at least a portion of their surface. Dilution of this suspension into a similar medium in which K-glutamate was replaced with 0.15 M choline chloride caused the complete disappearance of the crystal lattice within 15 to 30 sec (Fig. 5). Substitution of K-glutamate with choline chloride is expected to produce inside negative potential and it is assumed that the conformational change of the Ca^{2+}-ATPase under the influence of this potential is responsible for the disruption and disappearance of the Ca^{2+}-ATPase crystals.

The time course and magnitude of the potential were measured using the voltage sensitive dye Di–S–C_2(5) as indicator. Dilution of sarcoplasmic reticulum vesicles equilibrated in a K-glutamate medium into a medium containing choline chloride causes a decrease in the difference absorbance of Di–S–C_2(5) at 660 to 700 nm in response to negative potential; this is followed by a slow return of absorbance to near starting levels as the poten-

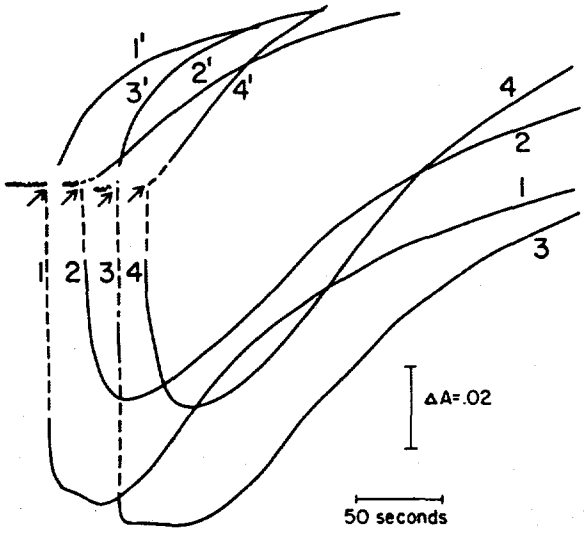

Fig. 6. Changes in the absorbance of $Di-S-C_2(5)$ after dilution of sarcoplasmic reticulum vesicles from K-glutamate into choline chloride medium. Sarcoplasmic reticulum vesicles (30 mg protein/ml) were equilibrated overnight at 2 °C in medium containing 0.15 M K-glutamate, 10 mM histidine (pH 6.8), 5 mM $MgSO_4$ and 50 μM $CaCl_2$. Inside negative potentials were generated by diluting 4 μl aliquots of this suspension into 2 ml of medium containing 0.15 M choline chloride, 10 mM histidine (pH 6.8), 5 mM $MgSO_4$, 10 μg/ml $Di-S-C_2(5)$, 1 μM valinomycin and: 50 μM $CaCl_2$ (trace 1); 50 μM $CaCl_2$, 5 mM Na_3VO_4 (trace 2); 1 mM EGTA (trace 3); 1 mM EGTA, 5 mM Na_3VO_4 (trace 4). The difference absorbance of $Di-S-C_2(5)$ at 660 to 700 nm was measured in an Aminco DW-2 spectrophotometer at 10 °C. For controls, the sarcoplasmic reticulum vesicles were equilibrated in choline chloride instead of K-glutamate and diluted as described above (traces 1'–4')

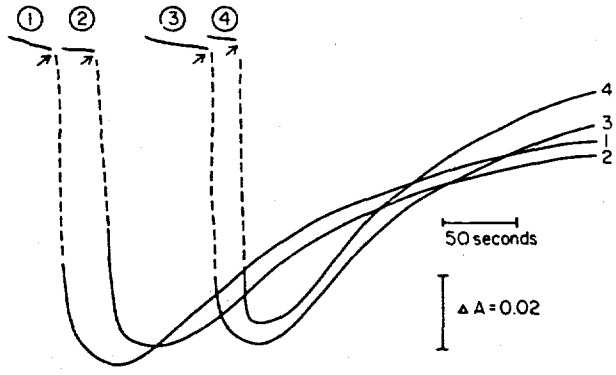

Fig. 7. Changes in absorbance of $Di-S-C_2(5)$ after dilution of sarcoplasmic reticulum vesicles from K-glutamate into choline chloride medium. Sarcoplasmic reticulum vesicles (30 mg protein/ml) were equilibrated overnight in a medium containing 0.15 M K-glutamate, 10 mM histidine pH 6.8, 5 mM $MgSO_4$, and either 50 μM $CaCl_2$ (samples 1 and 2) or 1 mM EGTA (samples 3 and 4). Samples 2 and 4 contained 5 mM Na_3VO_4. During incubation in the presence of EGTA and Na_3VO_4 (sample 4) Ca^{2+}-ATPase crystals develop while samples 1–3 serve as crystal-free controls. After overnight incubation the samples were diluted into media containing 0.15 M choline chloride, 10 mM histidine pH 6.8, 5 mM $MgSO_4$, 50 μM $CaCl_2$ and 10 μg ml $Di-S-C_2(5)$. The difference absorbance of $Di-S-C_2(5)$ was measured at the wavelength pair of 660 to 700 nm

tial is dissipated (Fig. 6, samples 1–4). Control samples diluted from choline-Cl into choline-Cl (Fig. 6, samples 1'–4') are not expected to generate potential and show only a slow increase in difference absorbance that is probably attributable to slow penetration of the dye into the vesicles. The rate of this change is much slower than the change observed under the influence of potential, and is not likely to affect significantly the conclusions. The magnitude of the absorbance change is greater in the absence (samples 1 and 3) than in the presence (samples 2 and 4) of vanadate whether the dilution medium contains 50 μM Ca (samples 1 and 2) or 1 mM EGTA (samples 3 and 4).

These observations suggest that Na_3VO_4 decreases the magnitude and duration of the potential change induced by ion substitution, presumably due to a change in the permeability of the membranes for ions.

There is no significant difference in the amplitude of the optical response between samples preincubated in the presence of 50 μM $CaCl_2$, that interferes with crystallization of the Ca^{2+}-ATPase (Fig. 7, samples 1, 2), and samples pre-incubated with 1 mM EGTA (Fig. 7, samples 3–4), that promotes crystallization of Ca^{2+}-ATPase in the presence of Na_3VO_4 (Fig. 7, sample 4). Therefore preexisting crystalline arrays of Ca^{2+}-ATPase do not affect the magnitude of potential change after transfer into choline chloride medium. The rate of disappearance of the optical response is slightly faster in samples containing 1 mM EGTA (Fig. 7, samples 3 and 4) in agreement with earlier observations (Duggan & Martonosi, 1970) that EGTA increases the permeability of sarcoplasmic reticulum membrane. This effect of EGTA is neutralized by Ca^{2+}.

Effect of Other Ion Substitutions

Transfer of vesicles from a Na-methanesulfonate solution into a medium containing K-methanesulfonate and 1 μM valinomycin also generates positive potential and promotes the crystallization of Ca^{2+}-ATPase (Dux & Martonosi, 1983*b*), while transfer from K-methanesulfonate solution into a

medium of Na-methanesulfonate + 1 μM valinomycin disrupts Ca^{2+}-ATPase crystals. Therefore the effects described in Figs. 1 through 6 are indeed attributable to changes in diffusion potential across the sarcoplasmic reticulum rather than to specific ion effects.

Discussion

Two effects of ion substitutions on the rate of crystallization of Ca^{2+}-ATPase were observed.

1. Transfer of vesicles from choline chloride into K-glutamate medium generates an inside positive potential across the vesicle membrane as indicated by a change in the absorbance of oxonol VI. The positive transmembrane potential favors the interaction between ATPase molecules with the formation of crystalline arrays of Ca^{2+}-ATPase in the presence of Na_3VO_4, presumably by changing the disposition of Ca^{2+}-ATPase in the membrane. Imposition of positive potential in the absence of Na_3VO_4 did not cause significant crystallization of Ca^{2+}-ATPase, although it inhibited the ATPase and Ca^{2+} transport activities of sarcoplasmic reticulum (Beeler et al., 1981). Therefore even in the absence of vanadate, transmembrane potential affects the conformation of the Ca^{2+}-ATPase in a functionally important manner.

The absorbance change of oxonol VI caused by ion substitution is generally smaller under conditions that promote the crystallization of Ca^{2+}-ATPase, raising the possibility that the vanadate-induced formation of Ca^{2+}-ATPase crystals increases the ion permeability of the membrane and facilitates the dissipation of transmembrane potential. A direct effect of vanadate upon the optical response of oxonol VI is observed even in the presence of Ca^{2+}, where crystallization cannot take place. The mechanism of this effect is not clear.

The crystalline arrays formed under the influence of positive potential usually occur on spherical vesicles in contrast to the elongated tubules that form after several days of crystallization. This may imply that the formation of tubular structures is a secondary, relatively slow process that follows the rapid crystallization.

2. Preformed crystalline arrays of Ca^{2+}-ATPase are disrupted when the microsome suspension is diluted from K-glutamate into choline chloride medium. Under these conditions an inside negative potential develops, as indicated by the absorbance change of $Di-S-C_2(5)$. The magnitude of the optical response is smaller in the presence than in the absence of vanadate in the dilution medium. However this difference cannot be attributed to crystallization of Ca^{2+}-ATPase since crystallization did not occur in media containing 50 μM Ca^{2+} and all crystals were destroyed upon dilution of vesicles from K-glutamate into choline chloride media. Na_3VO_4 may directly interfere with the optical response of $Di-S-C_2(5)$ or could produce other changes in the membrane not related to crystallization.

The disruption of Ca^{2+}-ATPase crystals by negative membrane potential is probably attributable to an effect on the conformation of the Ca^{2+}-ATPase that destabilizes ATPase-ATPase interactions. Since such interactions are presumed to take place in the E_2 conformation of the enzyme (Dux & Martonosi, 1983*a*), positive potential presumably favors the E_2 conformation, while negative potential would have the opposite effect.

Although active Ca^{2+} transport generates an inside positive potential (Beeler, 1980; Beeler et al., 1981), and a transient negative potential may arise during activated Ca^{2+} release (Beeler et al., 1981; Vergara & Bezanilla, 1981), there is no indication so far that these processes would be accompanied by changes in the monomer-polymer equilibrium of the Ca^{2+}-ATPase.

The work at the Uniformed Services University of the Health Sciences was supported by research grants GM29300 from the National Institutes of Health, and WR30241 from the Office of Naval Research. The work at SUNY Upstate Medical Center was supported by research grants AM26545 from the National Institutes of Health and by a grant-in-aid from the Muscular Dystrophy Association. Dr. Laszlo Dux was on leave from the Institute of Biochemistry, School of Medicine, University of Szeged, Hungary.

References

Beeler, T.J. 1980. Ca^{2+} uptake and membrane potential in sarcoplasmic reticulum vesicles. *J. Biol. Chem.* **255**:9156–9161

Beeler, T.J., Farmen, R.H., Martonosi, A. 1981. The mechanism of voltage-sensitive dye responses on sarcoplasmic reticulum. *J. Membrane Biol.* **62**:113–137

Bezanilla, F., Horowicz, P. 1975. Fluorescence intensity changes associated with contractile activation in frog muscle stained with Nile Blue A. *J. Physiol. (London)* **246**:709–735

Duggan, P.F., Martonosi, A.N. 1970. Sarcoplasmic reticulum. IX. The permeability of sarcoplasmic reticulum membranes. *J. Gen. Physiol.* **56**:147–167

Dux, L., Martonosi, A. 1983*a*. Two dimensional arrays of proteins in sarcoplasmic reticulum and purified Ca^{2+}-ATPase vesicles treated with vanadate. *J. Biol. Chem.* **258**:2599–2603

Dux, L., Martonosi, A. 1983*b*. The regulation of ATPase-ATPase interactions in sarcoplasmic reticulum. II. The influence of membrane potential. *J. Biol. Chem.* **258**:11903–11907

Jilka, R.L., Martonosi, A.N. 1977. The effect of calcium ion transport ATPase upon the passive calcium ion permeability of phospholipid vesicles. *Biochim. Biophys. Acta* **466**:57–67

Jilka, R.L., Martonosi, A.N., Tillack, T.W. 1975. Effect of the

purified [Mg^{2+} + Ca^{2+}]-activated ATPase of sarcoplasmic reticulum upon the passive Ca^{2+} permeability and ultrastructure of phospholipid vesicles. *J. Biol. Chem.* **250**:7511–7524

Martonosi, A. 1975. The mechanism of calcium transport in sarcoplasmic reticulum. *In:* Calcium Transport in Contraction and Secretion. E. Carafoli, F. Clementi, W. Drabikowski and A. Margreth, editors. pp. 313–327. North-Holland, Amsterdam

Martonosi, A., Nakamura, H., Jilka, R.L., Vanderkooi, J.H. 1977. Protein-protein interactions and the functional states of sarcoplasmic reticulum membranes. *In:* Biochemistry of Membrane Transport. G. Semenza and E. Carafoli, editors. pp. 401–415. Springer, Berlin

Nakamura, H., Jilka, R.L., Boland, R., Martonosi, A. 1976. Mechanism of ATP hydrolysis by sarcoplasmic reticulum and the role of phospholipids. *J. Biol. Chem.* **251**:5414–5423

Taylor, K.A., Dux, L., Martonosi, A. 1983. Oligomer structure of the Ca^{2+}-ATPase from sarcoplasmic reticulum. *Fed. Proc.* **42**:1933

Vanderkooi, J.M., Ierokomos, A., Nakamura, H., Martonosi, A. 1977. Fluorescence energy transfer between Ca^{2+} transport ATPase molecules in artificial membranes. *Biochemistry* **16**:1262–1267

Vergara, J., Bezanilla, F. 1981. Optical studies of E–C coupling with potentiometric dyes. *In:* The Regulation of Muscle Contraction: Excitation Contraction Coupling. A.D. Grinnell and M.A.B. Brazier, editors. pp. 67–77. Academic Press, New York

Received 17 June 1983; revised 30 August 1983